Atmospheric Environment 51 (2012) 146–164

Contents lists available at SciVerse ScienceDirect

Atmospheric Environment

journal homepage: www.elsevier.com/locate/atmosenv

Assessing sensitivity regimes of secondary inorganic aerosol formation in Europe with the CALIOPE-EU modeling system

María T. Pay [a], Pedro Jiménez-Guerrero [b], José M. Baldasano [a,c,*]

[a] Earth Sciences Department, Barcelona Supercomputing Center-Centro Nacional de Supercomputación, Barcelona, Spain
[b] Physics of the Earth, University of Murcia, Spain
[c] Environmental Modeling Laboratory, Technical University of Catalonia, Barcelona, Spain

ARTICLE INFO

Article history:
Received 19 July 2011
Received in revised form
11 January 2012
Accepted 12 January 2012

Keywords:
Air quality
Model evaluation
Aerosol precursors
Geochemistry
Sulfate
Nitrate
Ammonia

ABSTRACT

Sulfur dioxide and nitrogen oxides form two of largest contributors to PM2.5 in Europe; ammonium sulfate ($(NH_4)_2SO_4$) and ammonium nitrate (NH_4NO_3). In-situ observations of many chemical components are rather sparse, and thus neither can accurately characterize the distribution of pollutants nor predict the effectiveness of emission control. Understanding (and controlling) the formation regimes for these components is important for the achievement of the reduction objectives established in the European legislation for PM2.5 (20% of PM2.5 triennial for the mean of urban background levels between 2018 and 2020). For this purpose, the present work uses the CALIOPE high-resolution air quality modeling system (12 km × 12 km, 1 h) to investigate the formation of SIA (SO_4^{2-}, NO_3^- and NH_4^+, which involve an important part of PM) and their gaseous precursors (SO_2, HNO_3 and NH_3) over Europe during the year 2004. The CALIOPE system performs well at estimating SIAs when compared to the measurements from EMEP monitoring network, but errors are larger for gaseous precursors. NH_3 is underestimated in the warmest months, HNO_3 tends to be overestimated in the summer months, and SO_2 appears to be systematically overestimated. The temporal treatment of ammonia emission is a probable source of uncertainty in the model representation of SIA. Furthermore, we discuss the annual pattern for each inorganic aerosol and gas precursor species over Europe estimated with the EMEP data and CALIOPE outputs, comparing the performance with other European studies. Spatial distribution of key indicators is used to characterize chemical regimes and understand the sensitivity of SIA components to their emission precursors. Results indicate that SO_4^{2-} is not usually fully neutralized to ammonium sulfate in ambient measurements and is usually fully neutralized in model estimates. CALIOPE and EMEP observations agree that the continental regions in Europe tend to be HNO_3-limited for nitrate formation. Regulatory strategies in such regions should focus on reductions in NO_x ($NO + NO_2$) rather than NH_3 to control ammonium nitrate. This work assesses how well the CALIOPE system reproduces the spatial and temporal variability of SIAs and their gaseous precursors over Europe and complements the measurement findings.

1. Introduction

Atmospheric PM, or aerosols, plays a central role in atmospheric processes (Fountoukis and Nenes, 2007). They have adverse effects on human health (Pope et al., 2009) and affect visibility (Altshüller, 1984), ecosystems (Niyogi et al., 2004; Bytnerowicz et al., 2007), air quality and climate change (IPCC, 2007). To alleviate some of these atmospheric problems, the control of atmospheric PM concentration

Abbreviations: PM2.5, particles with a diameter < 2.5 μm; CALIOPE, WRF-ARW/EMEP-HERMES/CMAQ/BSC-DREAM8b; SIA, secondary inorganic aerosol; PM, particulate matter; EMEP, European Monitoring and Evaluation Programme; PM10, particles with a diameter < 10 μm; NMVOC, non methane organic volatile compounds; CTM, Chemical Transport Model; WRF-ARW, Advanced Research Weather Research and Forecasting Model; HERMES-EMEP, High-Elective Resolution Modeling Emission System-European Monitoring and Evaluation Programme; CMAQ, Models-3 Community Multiscale Air Quality Modeling System; BSC-DREAM8b, Dust REgional Atmospheric Model version 8 bins developed at the Barcelona Supercomputing Center – Centro Nacional de Supercomputación; CALIOPE-EU, The CALIOPE system applied over the European domain in 2004; CB-IV, Carbon Bond IV; SNAP, Selected Nomenclature Air Pollution; EPER, European Pollutant Emission Register; ESRI, Environmental System Research Institute; MSC-W, Meteorological Synthesizing Centre-West; MB, mean bias; RMSE, root mean square error; *r*, correlation coefficient; MFB, mean fractional bias; MFE, mean fractional error; Ratio, the ratio between modeled mean and observed mean.

* Corresponding author. Earth Sciences Department, Barcelona Supercomputing Center-Centro Nacional de Supercomputación (BSC-CNS), Jordi Girona 29, Edificio Nexus II, 08034 Barcelona, Spain. Tel.: +34 93 413 77 19; fax: +34 93 413 77 21.
E-mail address: jose.baldasano@bsc.es (J.M. Baldasano).

1352-2310/$ – see front matter © 2012 Elsevier Ltd. All rights reserved.
doi:10.1016/j.atmosenv.2012.01.027

is needed. European legislation has established regulations regarding PM10 and recently for PM2.5 in order to reduce human exposure to high concentration of PM (European Commission, 2008).

PM is both emitted directly from a large variety of anthropogenic, biogenic and natural sources and formed in the atmosphere by chemical and physical processes from gas-phase precursors such as NMVOC, NO_x, SO_2 and NH_3 (Seinfeld and Pandis, 1998). Therefore, to fulfill the task of reducing human exposure to PM, policies must focus not only on the reduction of primary particulate emissions, but also on the reduction of precursor emissions for the formation of secondary particles (Wu et al., 2008; Renner and Wolke, 2010). With this purpose, in Europe within the National Emission Ceiling (NEC) directive and the multi-pollutant and multi-effect Gothenburg protocol, national emission ceilings for SO_2, NO_x, NH_3 and VOC have been agreed upon to reduce acidification and eutrophication effects and to reduce human exposure to ozone.

Several experimental studies have analyzed levels, speciation and origin of PM over Europe (Querol et al., 2004, 2009; van Dingenen et al. 2004; Putaud et al., 2004, 2010). They found that the European background levels, derived form 31 European air monitoring stations, have been 7.0 ± 4.1 μg PM10 m^{-3} and 4.8 ± 2.4 μg PM2.5 m^{-3}, over the past decade. The observed aerosol composition reveled that organic matter is a major component in PM10 and PM2.5, except at rural background sites where SIA contribution prevailed. The dominant SIA species are ammonium sulfates and ammonium nitrates salts.

The formation of SIA is a two-step process. First, the primary emissions of NO_x and SO_2 are oxidized to form nitric acid (HNO_3) and sulfuric acid (H_2SO_4), respectively, precursors of secondary aerosols. Secondly, H_2SO_4, HNO_3 and NH_3 partitions between the gas and particle phase according to thermodynamic equilibrium determined by temperature, relatively humidity and molar concentration of SO_4^{2-}, total nitrate ($TNO_3 = HNO_3 + NO_3^-$) and total ammonia ($TNH_3 = NH_3 + NH_4^+$). SO_2 emissions in Europe have been reduced ~67% from 1980 to 2000 (EMEP, 2004; Fagerli and Aas, 2008; Hamed et al., 2010). Thus, nowadays less NH_3 is converted to $(NH_4)_2SO_4$ and more NH_3 is available for the formation of NH_4NO_3. This situation leads to a higher residence time of TNO_3 in air (Fagerli and Aas, 2008).

Because of the complex relationship between SIAs (Ansari and Pandis, 1998; Vayenas et al., 2005) the control of PM2.5 is still nowadays a difficult challenge. In this sense, CTMs are important tools for air quality assessment and the evaluation of emission control policies, but it becomes necessary to assess their ability in simulating pollution quality levels. Single model evaluation studies (Schaap et al., 2004a; Sartelet et al., 2007; Stern et al., 2008; Matthias, 2008), model inter-comparisons (Hass et al., 2003; van Loon et al., 2004); and model ensembles (Vautard et al., 2009) showed that models tend to underestimate observed PM and their SIA components. The results of these studies show large uncertainties in the estimation of the meteorological input data, uncertainties in the modeling of the anthropogenic PM sources, missing natural and biogenic sources and also with gaps in the knowledge of many of the physical and chemical processes which lead to the formation of SIA.

The main purpose of this work is to characterize SIA formation regimes and understand the sensitivity of SIA vs. their gaseous counterpart over Europe by means of the CALIOPE air quality modeling system (Pay et al., 2010a; Baldasano et al., 2011) with a simulation covering the whole year 2004. This paper is structured as follows. Section 2 describes the modeling system, the observational database and the evaluation tools. Section 3 analyses the modeling results against available measured data for the year 2004 and discusses the modeled and observed annual patterns of SIA and their gas-precursors. Also a discussion about aerosol formation regimes over Europe is provided. Section 4 presents a thorough comparison of statistical evaluation results with other European studies. Finally, conclusions are drawn in Section 5.

2. Methods

2.1. Model description and setup

CALIOPE (Baldasano et al., 2008a) is a complex system that integrates a meteorological model (WRF-ARW), an emission processing model (HERMES-EMEP), a CTM (CMAQ) and a mineral dust dynamic model (BSC-DREAM8b) together coupled in an air quality modeling system (Fig. 1 of Pay et al., 2010a). CALIOPE encompasses a high-resolution air quality modeling system which provides 48-h air quality forecasts in Europe (12 km × 12 km) and Spain (4 km × 4 km) (available at: www.bsc.es/caliope). The system has been widely evaluated during its development over northeastern Spain (Jiménez et al., 2005a,b, 2006a,b, 2007), the Iberian Peninsula (Jiménez-Guerrero et al., 2008a; Baldasano et al., 2008a, 2011; Pay et al., 2010b) and Europe (Pay et al., 2010a). Furthermore, it has been used for assessing air pollution dynamics (Gonçalves et al., 2009a) and as management tool to study air quality impact of urban management strategies (Jiménez-Guerrero et al., 2008b; Gonçalves et al., 2008, 2009b; Soret et al., 2011).

The CALIOPE system applied over the European domain in 2004 is namely hereafter as CALIOPE-EU. For a detailed description of the modeling system we refer to aforementioned studies. Here, we describe the most relevant model characteristics and the setup used in this study.

Meteorological input data for the CMAQ model are processed using the WRF-ARW model version 3.6.1 (Michalakes et al., 2004; Skamarock and Klemp, 2008). Details about the performance of WRF-ARW over the European domain are provided as supplementary material.

The CMAQ model version 4.5 is a three-dimensional Eulerian CTM that uses state-of-the-science routines to model gas and particulate matter formation and removal processes (Byun and Schere, 2006; Appel et al., 2008; Roy et al., 2007). The gas-phase oxidations in the atmosphere are described in the CB-IV chemical mechanism (Gery et al., 1989) following the criteria of Jiménez et al. (2003). Aerosols are represented by the modal aerosol module AERO4 (Binkowski and Roselle, 2003) which contains a preliminary treatment of sea salt emissions and chemistry (Bhave et al., 2005; Shankar et al., 2005). Three log-normal modes spanning three size categories Aitken (0.01–0.1 μm diameter), accumulation (0.1–1 μm) and coarse (>1 μm). The aerosol within each model is internally mixed.

Fine-particle SO_4^{2-} has an anthropogenic origin and is directly emitted, generated by nucleation and/or condensation from the gas phase oxidation of SO_2 and hydroxyl radical (OH) and by heterogeneous oxidation of SO_2 in clouds (Binkowski and Roselle, 2003). The effective cloud SO_2 oxidation rate in CMAQv4.5 depends primarily on cloud liquid water content, the presence of species affecting pH (e.g., HNO_3 and NH_3), concentration of O_3 and H_2O_2 and cloud lifetime. Under optimal conditions clouds can effectively convert all ambient SO_2 into sulfate within the volume of air they process. The cloud-cover metric (fraction of total sky covered by clouds near or just above the top of the PBL) determinates heterogeneous SO_2 oxidation. The three-dimensional WRF-ARW fields of cloud water mixing ration determine the presence of resolved cloud layers in CMAQ. In CMAQv4.5 cloud treatment follows the asymmetric convective module (Pleim and Chang, 1992).

HNO_3 is produced by heterogeneous hydrolysis of N_2O_5 and by gas-phase oxidation of NO_x by OH. Atmospheric H_2SO_4 is neutralized by NH_3 to form $(NH_4)_2SO_4$. Remaining NH_3 (further denoted as free ammonia) may then combine with HNO_3 to form the semi-volatile NH_4NO_3. This equilibrium is function of ambient

conditions (temperature, relative humidity) and the precursor concentrations. The AERO4 module uses the gas/aerosol partitioning treated using the ISORROPIA thermodynamic module (Nenes et al., 1999).

Note that the model does not include the formation of coarse mode nitrate through reaction of nitric acid or sulfuric acid with sea salt or dust.

The CALIOPE-EU system, as the most European CTMs, uses the EMEP inventory of the anthropogenic emissions of SO_2, NO_x, NMVOC, CO, PM, and NH_3 (http://www.ceip.at/emission-data-webdab/) which contains annual emissions (year 2004 in this study) for 11 SNAP sectors by countries in a 50 km × 50 km grid.

Disaggregation method of the annual EMEP inventory is performed in space (12 km × 12 km in horizontal, 15σ layers in vertical) and time (1 h) and it distinguishes between SNAP sectors. In the horizontal dimension, emission data are mapped applying different criteria through three datasets: (1) high-resolution land use map (EEA, 2000), (2) coordinates of industrial sites (EPER), and (3) vectorized road cartography of Europe (ESRI). On the other hand, the CALIOPE-EU system, as most European CTMs use the emission vertical distribution profiles from the EMEP model (Vidic, 2002; Simpson et al., 2003, http://www.emep.int/UniDoc/node7.html) for SO_2 and the other gaseous anthropogenic emissions. These profiles are based on five years of plume rise calculations for the city of Zagreb, Croatia. These vertical profiles are based on rough estimates because (1) they may not be representative for other European regions, (2) they are applied over a coarse vertical resolution of 6 layers between 92–1100 m does not match the resolution used for CALIOPE (which has 15 sigma layers, with 11 layers between 19.5–1025 m), and (3) they are annual averages and they do not consider the diurnal and seasonal cycles. Some studies (de Meij et al., 2006; Pregger and Friedrich, 2009; Bieser et al., 2011a) indicate that the vertical distribution of these emissions have a large effect on the concentrations calculated by CTM because it influences the chemical composition of air and removal and transport of substances, as an example, the formation of secondary pollutants, such as SO_4^{2-} from SO_2 (Bieser et al., 2011b).

In the time dimension, emission data are temporally distributed per source sector using time factors: monthly, daily and hourly consecutively. Temporal correction factors are derived from EMEP/MSC-W, provided by the Institute of Energy Economics and the Rational Use of Energy (IER) of the University of Stuttgart.

Biogenic emissions are estimated internally as a function of temperature, radiation and land-use following Baldasano et al. (2008a,b).

Fig. 1 and Table 1 show the annual averaged emissions of the most contributed sectors of the emitted compounds SO_x, NO_x, NH_3 and NMVOC in Europe. In 2004, 56% of the total SO_x emissions were attributed to energy transformation. 64% of NO_x total emissions are attributed to transport (road and no-road, sector 7 and 8). 94% of NH_3 total emissions are attributed to agriculture and livestock. Domestic animals contribute most to total emissions, followed by fertilizers, crops and others. 33% of NMVOC total emissions are attributed to on-road transport and other 33% to the use of solvents. Last, 50% of CO total emissions are attributed to on-road transport.

The photochemical modeling domain consists of 479 cells in the *X* direction and 399 cells in the *Y* direction covering the European domain with 12 km × 12 km grid cells in a Lambert projection. The CMAQ horizontal grid resolution corresponds to that of WRF-ARW. Its vertical structure was obtained by a collapse from the 38σ-WRF-ARW layers to a total of 15 σ-layers steadily increasing from the surface up to 50 hPa with a stronger concentration within the PBL. The chemical boundary conditions are based on the global climate chemistry model LMDz-INCA2 (Piot et al., 2008; Szopa et al., 2009).

2.2. Air quality network for gas and aerosol phase

Model output for SIA and gaseous precursor concentrations are compared with ground-based measurements of SO_2, SO_4^{2-}, HNO_3, NO_3^-, NH_3, NH_4^+, $TNO_3(NO_3^- + HNO_3)$ and $TNH_3(NH_4^+ + NH_3)$ from the EMEP monitoring network for the year 2004. EMEP stations are assumed to be representative of regional background concentrations (Torseth and Hov, 2003). The authors wish to stress that the model performances presented in this paper are evaluated only for background concentrations. EMEP has an extensive quality control of the data that are included in the database, freely available on its web page (http://www.emep.int). However, accurate measurements of SIA aerosol remain a challenge. Inorganic species may be measured with an uncertainty of about ±10% for major species (Putaud et al., 2004). Filter-packs are typically used to measure long-term data on SIA components at EMEP sites and subsequent chemical analysis. The volatile character of NH_4NO_3 and the reactivity of HNO_3 make these filtration methods prone to artifacts. The evaporation artifact leads to serious underestimation of ambient concentration, especially during summer (Schaap et al., 2004b; Vecchi et al., 2009). Despite of the evaporation artifacts the actual nitrate concentration can also be overestimated depending on the filter type. Cellulose type aerosol filter, commonly used in Europe, retain HNO_3 which is thus assigned to aerosol NO_3^- (Schaap et al., 2004b).

All EMEP measurement data are given as daily average. As a result, 31 stations were selected to evaluate SO_2, 53 for SO_4^{2-}, 8 for HNO_3, 31 for NO_3^-, 7 for NH_3, and 15 for NH_4^+, for respectively. SIA and gas precursors are also indirectly evaluated with measurements of TNO_3 and TNH_3 available at 31 stations. The selected EMEP stations and measured pollutants that are used for this comparison are briefly described in Table 2 and presented in Fig. 2. Note that the final coverage of the dataset is rather uneven since France, Italy and southeastern Europe only include several stations. In the case of nitrogenous gas precursors (HNO_3 and NH_3) is remarkable the limited number of stations and their irregular distribution.

2.3. Evaluation and assessment tools

EMEP observations for sulfate, nitrate, and ammonium usually include particles with aerodynamic diameters less than 10 μm due to the fact that measurements are typically performed with filter-packs. Modeled SIA are post-processed for the comparison with EMEP observations. A list of CMAQ aerosol module variables can be found in Table 1 of Binkowski and Roselle (2003). To compare with EMEP observations, total concentrations of SO_4^{2-}, NO_3^-, and NH_4^+ are approximated by summing the appropriate Aitken- and accumulation-mode concentrations. As the CALIOPE-EU system estimates coarse sulfate from sea salt, total modeled sulfate also takes into account marine contribution to be compared with observations, hereafter referred to as SO_4^{2-}.

To account for the sub-grid variability of concentrations a bilinear interpolation is applied to the model output, since EMEP measurements are representative of regional background concentrations. Measurements are on a daily basis, thus aerosols are compared in terms of daily averages from the modeling system.

Metrics used to describe the modeling system performance include classical statistics. Besides mean of modeled and measured values we show MB, RMSE, *r*, MFB, and MFE (Boylan and Russell, 2006; Dennis et al., 2010). The bias and error describe the performance in terms of the measured concentration units ($\mu g\,m^{-3}$) assuming that measurements are the truth. On the other hand, fractional metrics describe model performance normalizing for each model-observed pair by the average of the model and observation, considering that measurements have their own uncertainty due to biases and artifacts related to sampling and laboratory analysis

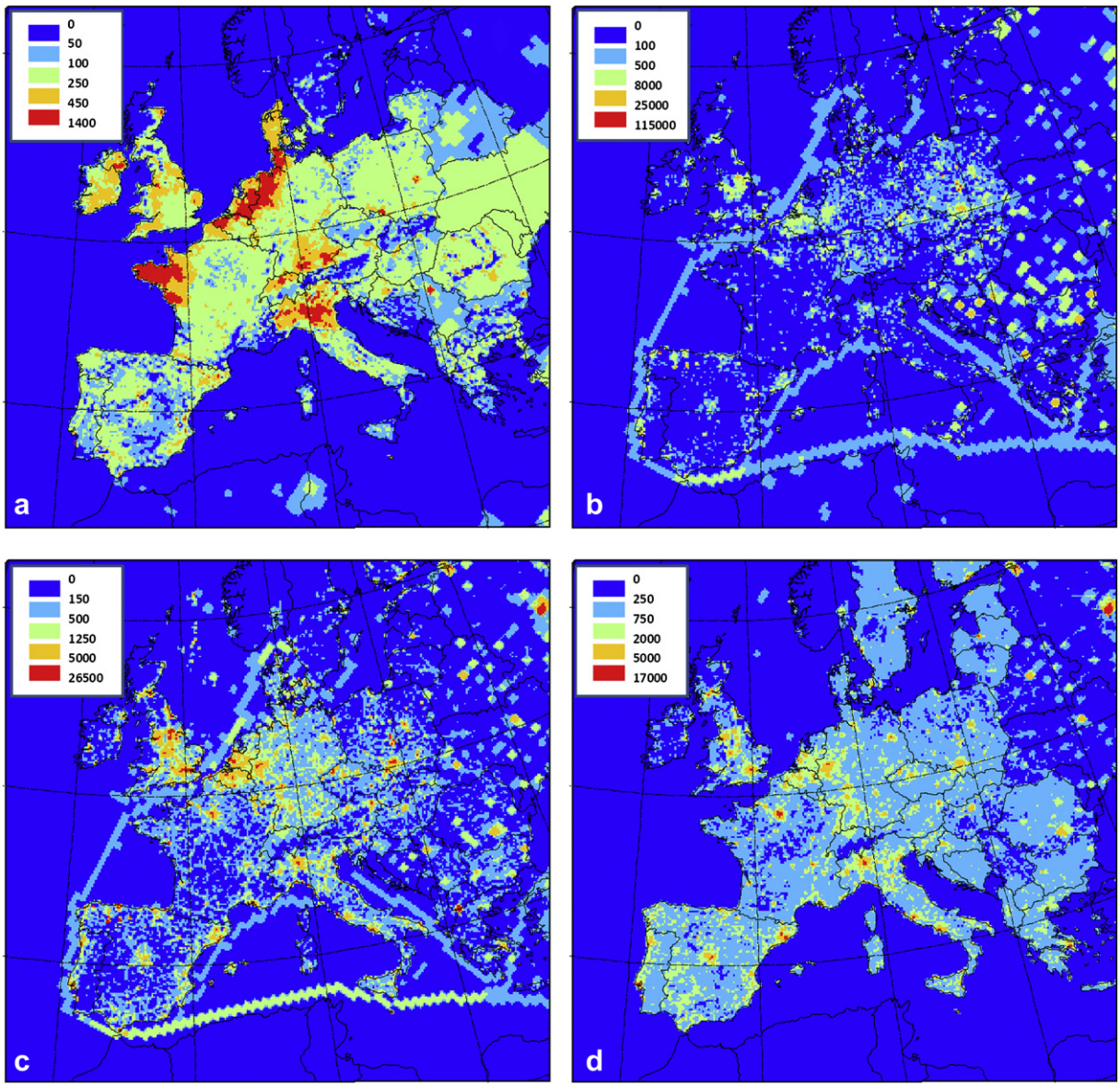

Fig. 1. Distribution of the anthropogenic emission (in Mg yr^{-1}) of: NH_3 (a), SO_x (b), NO_x (c), NMVOC (d) for the year 2004 in Europe.

methods (Boylan and Russell, 2006; Putaud et al., 2010). The best model performance is when MFB and MFE approach 0. The fractional metrics are bounded by 200%, which is considered very poor performance. The fractional bias and error metrics normalize large and small concentrations, making seasonal trends in model performance more discernable.

The bias metrics between SIAs and gas-phase precursors are examined for relationships to determined how much of the error in

Table 1
Total emission of SO_x, NO_x, NMVOC, PM2.5, PM coarse, CO and NH_3 for the year 2004 for anthropogenic activities in Europe aggregated by SNAP (Selected Nomenclature Air Pollution) category (in Mg yr^{-1}).

SNAP	Description	SO_x	NO_x	NMVOC	PM2.5	PM coarse	CO	NH_3
1	Energy transformation	9323	3483	137	295	386	852	7
2	Small combustion sources	1161	1028	1163	825	314	10,803	7
3	Industrial combustion	2096	2096	180	299	202	5499	6
4	Industrial process	734	385	1504	552	315	3643	106
5	Extraction of fossil fuels	0	0	0	0	0	0	0
6	Solvent and product use	0	0	4300	21	11	22	5
7	Road transport	314	6491	4355	361	95	26,001	82
8	Non road transport	2868	6166	754	487	57	3115	2
9	Waste handling and disposal	25	41	159	97	15	1832	143
10	Agriculture	2	246	508	176	332	535	5823
	Total	16,522	19,937	13,059	3113	1727	52,303	6182

Table 2
Coordinates, altitude and measured chemical species at the 54 selected EMEP stations. The code is composed by 2-letter country code plus 2-digit station code. Zone is defined as follows: Western Iberian Peninsula (W.IP); Eastern Iberian Peninsula-Western Mediterranean (E.IP-W.Med), Central Mediterranean (C.Med), Eastern Mediterranean (E.Med), North of Italy (N. It.), Eastern Europe (E.Eu), Northwestern Europe (NW.Eu), Southern France (S.Fr.), Central Europe (C.Eu), Nordic (Nord), Central France (C.Fr) and North Atlantic (N.Atl).

	Station name	Station code[a]	Zone	Lat.[b]	Lon.[b]	Alt. (m)	SO_4^{2-}	NO_3^-	NH_4^+	NH_3	HNO_3	TNH_3	TNO_3	SO_2
1	Anholt	DK08	Nord	+56.717	+11.517	40	×					×	×	×
2	Barcarrota	ES11	W.IP	+38.476	−6.923	393	×	×				×	×	×
3	Birkenes	NO01	Nord	+58.383	+8.250	190	×	×	×	×	×	×	×	
4	Cabo de Creus	ES10	E.IP-W.Med	+42.319	+3.317	23	×	×				×	×	
5	Campisábalos	ES09	W.IP	+41.281	−3.143	1360	×	×		×		×	×	×
6	Chopok	SK02	E.Eu	+48.933	+19.583	2008	×							
7	Deuselbach	DE04	NW.Eu	+49.767	+7.050	480	×					×	×	
8	Diabla Gora	PL05	E.Eu	+54.150	+22.067	157	×					×	×	
9	Donon	FR08	C.Eu	+48.500	+7.133	775	×							×
10	Els Torms	ES14	E.IP-W.Med	+41.400	+0.717	470	×	×				×	×	×
11	Eskdalemuir	GB02	NW.Eu	+55.313	−3.204	243	×							
12	High Muffles	GB14	NW.Eu	+54.334	−0.808	267	×							
13	Illmitz	AT02	E.Eu	+47.767	+16.767	117	×	×	×	×	×			×
14	Iraty	FR12	S.Fr	+43.033	−1.083	1300	×							×
15	Iskrba	SI08	N.It	+45.567	+14.867	520	×					×	×	
16	Ispra	IT04	N.It	+45.800	+8.633	209	×	×	×					
17	Jarczew	PL02	E.Eu	+51.817	+21.983	180	×	×	×			×	×	×
18	Jungfraujoch	CH01	C.Eu	+46.550	+7.983	3573	×	×	×					
19	Kollumerwaard	NL09	NW.Eu	+53.334	+6.277	1		×	×					
20	Kosetice	CZ03	E.Eu	+49.583	+15.083	534	×					×	×	×
21	K-puszta	HU02	E.Eu	+46.967	+19.583	125	×	×	×	×	×			
22	La Tardière	FR15	C.Fr	+46.650	+0.750	746	×							
23	Le Casset	FR16	C.Eu	+45.000	+6.467	746	×							
24	Leba	PL04	Nord	+54.750	+17.533	2	×	×	×			×	×	×
25	Liesek	SK05	E.Eu	+49.367	+19.683	892	×	×			×			
26	Lough Navar	GB06	N.Atl	+54.443	−7.870	126	×							
27	Melpitz	DE44	NW.Eu	+52.530	+12.93	86	×	×	×					
28	Montandon	FR14	C.Eu	+47.183	+6.500	746	×							
29	Montelibretti	IT01	C.Med	+42.100	+12.633	48	×	×	×	×	×			×
30	Morvan	FR10	C.Fr	+47.267	+4.083	620	×							
31	Niembro	ES08	W.IP	+43.442	−4.85	134	×	×		×		×	×	×
32	O Savñao	ES16	W.IP	+42.653	−7.705	506	×	×				×	×	×
33	Payerne	CH02	C.Eu	+46.817	+6.950	510	×					×	×	
34	Penausende	ES13	W.IP	+41.283	−5.867	985	×	×				×	×	×
35	Peyrusse Vieille	FR13	S.Fr	+43.375	+0.104	236	×							×
36	Preila	LT15	Nord	+55.350	+21.067	5	×					×	×	×
37	Råö	SE14	Nord	+57.400	+11.917	5	×					×	×	
38	Revin	FR09	NW.Eu	+49.900	+4.633	390	×							×
39	Rigi	CH05	C.Eu	+47.069	+8.466	1030	×					×	×	×
40	Risco Llamo	ES15	W.IP	+39.517	−4.350	1241	×	×				×	×	×
41	Rucava	LV10	Nord	+56.217	+21.217	5	×	×	×			×	×	×
42	Skreådalen	NO08	Nord	+58.817	+6.717	475	×	×	×	×	×	×	×	
43	Sniezka	PL03	E.Eu	+50.733	+15.733	1603	×	×	×			×	×	×
44	Starina	SK06	E.Eu	+49.050	+22.267	345	×	×			×			×
45	Svratouch	CZ01	E.Eu	+49.733	+16.033	737	×					×	×	×
46	Tange	DK03	Nord	+56.350	+9.600	13	×					×	×	×
47	Topolniky	SK07	E.Eu	+47.960	+17.861	113	×	×			×			
48	Utö	FI09	Nord	+59.779	+21.377	7	×		×			×	×	
49	Valentina Observatory	IE01	N.Atl	+51.94	−10.244	11	×					×	×	
50	Vavihill	SE11	Nord	+56.017	+13.150	175	×					×	×	×
51	Víznar	ES07	E.IP-W.Med	+37.233	−3.533	1265	×	×				×	×	
52	Yarner Wood	GB13	NW.Eu	+50.596	−3.713	119	×							
53	Zarra	ES12	E.IP-W.Med	+39.086	−1.102	885	×	×				×	×	×
54	Zoseni	LV16	Nord	+57.133	+25.917	183	×	×	×			×	×	×

[a] 2-Letter country code plus 2-digit station code.
[b] A positive value indicates northern latitudes or eastern longitudes. A negative value indicates southern latitudes or western longitudes.

precursor model performance translates into error for co-located ion model estimates. Besides, to characterize SIA formation regimes and understand the sensitivity of SIAs to their gaseous counterparts, we introduce three indicators. *S*-ratio (Hass et al., 2003) (Eq. (1)) indicates the ability of the model to form the sulfate aerosols. Concentrations are expressed as $\mu g\, m^{-3}$ in the *S*-ratio equation.

$$S - \text{ratio} = \frac{SO_2}{SO_2 + SO_4^{2-}} \quad (1)$$

SO_4^{2-} is produced during the transport by heterogeneous processes in clouds. A ratio close to unity indicates that only a small fraction of the emitted SO_2 has been converted to the sulfate aerosol.

Free ammonia (F-NH_x) (Eq. (2)) indicator quantifies the amount of ammonia available, after neutralizing SO_4^{2-}, for NH_4NO_3 formation. This indicator is based on the fact that $(NH_4)_2SO_4$ aerosol is the favored form for sulfate. F-NH_x is defined as the total ammonia minus twice the sulfate concentration on a molar basis:

$$F - NH_x = TNH_3 - 2SO_4^{2-} \quad (2)$$

The gas–aerosol equilibrium in the $SO_4^{2-}/NO_3^-/NH_4^+$ system is analyzed using the *G*-ratio (Ansari and Pandis, 1998; Pinder et al., 2008)

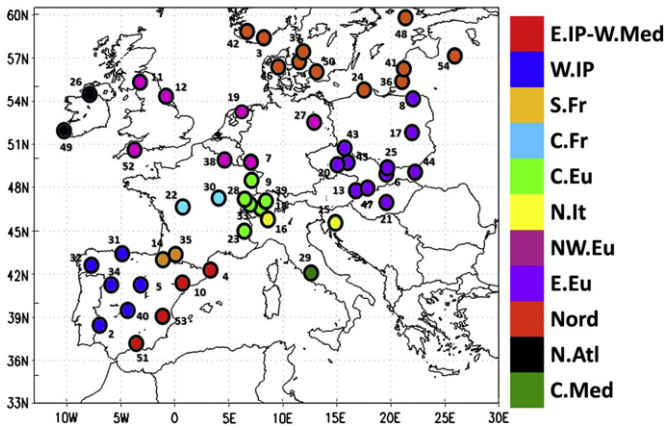

Fig. 2. Spatial distribution of 54 selected EMEP stations over the study domain. The different colors indicate the different zones defined in Table 2. Number of each station is listed in Table 2.

(Eq. (3)) which indicates whether fine-particle NO_3^- formation is limited by the availability of HNO_3 or NH_3. All the terms in the following equation are expressed molar basis ($\mu mole\ m^{-3}$).

$$G-\text{ratio} = \frac{F-NH_x}{TNO_3} \quad (3)$$

G-ratio > 1 indicates that nitric acid is limiting, while G-ratio < 0 indicates the ammonia is severely limiting. G-ratio between 0 and 1 indicates ammonia is available for reaction with nitric acid, but ammonia is the limiting species.

Pinder et al. (2008) suggested an adjust G-ratio which takes into account that sulfate is not always fully neutralized. That is true especially during wintertime when ammonia emissions are still high enough. However, we decided not to use this adjust G-ratio since only 5 stations are available to evaluate the modeled pattern.

3. Results and discussion

First, the CALIOPE system is evaluated in terms of statistical indicators in Section 3.1. Fig. 3 compares the CALIOPE-EU model outputs with measurements for inorganic aerosols (SO_4^{2-}, NO_3^- and NH_4^+) and their precursors (SO_2, HNO_3 and NH_3) computed on a daily basis using all the EMEP stations with available data. Also, Fig. 4 shows the monthly MFB and MFE for each species (gas and precursor) compared to proposed performance goals and criteria by Boylan and Russell (2006). Second, in Section 3.2, a general description of the annual mean distribution of each pollutant is provided to determine each pattern across Europe (Fig. 5). Latter, Section 3.3 the discussion is focused on the use of indicators that allow detecting SIA formation regimes over Europe (Figs. 6–8).

3.1. Model evaluation

3.1.1. Sulfur dioxide and sulfate

For SO_2, the model results are evaluated against 31 stations located across the Iberian Peninsula, central and north-eastern Europe. Fig. 3a shows the modeled SO_2 temporal evolution which is able to reproduce the annual variation of daily measurements ($r = 0.60$) although it overestimates some observed peaks (MB $= 0.5\ \mu g\ m^{-3}$). As shown in Fig. 4a and b bias and errors for SO_2 do not present a significant seasonal variation. Monthly biases are relatively low ($0\% <$ MFB $< 30\%$) and fall within the performance goal proposed by Boylan and Russelle (2006). Nevertheless monthly fractional errors only accomplish the criteria ($60\% <$ MFE $< 75\%$).

Modeled SO_4^{2-} concentrations are evaluated at 53 EMEP stations which cover Spain, eastern and central Europe and Nordic countries. The annual variability of the modeled SO_4^{2-} concentrations agrees fairly well with measurements ($r = 0.49$, RMSE $= 1.3\ \mu g\ m^{-3}$) and modeling results present a low negative bias along the year (MB $< -0.3\ \mu g\ m^{-3}$) (Fig. 3b). Best model performances are achieved during warm seasons (MFB $\sim$ 0% and MFE $\sim$50%, Fig. 4a and b) when ambient concentrations are highest due to enhanced photochemistry, low air mass renovation regional scale, and the increase of the summer mixing layer depth favoring the regional mixing of polluted air masses (Querol et al., 2009). Only during cold seasons SO_4^{2-} from CALIOPE-EU does not accomplish the goal for MFB and MFE. This result is geographically biased by winter underestimations at eastern European stations (E. Eu region), where MB by station ranges from $-0.5\ \mu g\ m^{-3}$ to $-2.5\ \mu g\ m^{-3}$.

January and March undergo three major episodes of enhanced SO_2 and SO_4^{2-}. The model reproduces accurately the SO_2 variability meanwhile sulfate events are not reproduced. Overall, the positive mean bias only for SO_2 suggests that SO_4^{2-} formation in the modeling system is often limited by oxidant availability and not always by SO_2 availability. Winter underestimation of SO_4^{2-} is a common issue in most models which operate over Europe which represent a direct couplet of sulfur chemistry with photochemistry, even detected with CMAQ over Europe (Matthias, 2008). This feature can be probably explained by a lack of model calculated oxidants or missing reactions (Kasibhatla et al., 1997). In this context, besides the gas phase reaction of SO_2 by OH, Tarrasón and Iversen (1998) and Schaap et al. (2004a) included additional oxidation pathways in clouds under cool and humid conditions that improve modeled SO_4^{2-} performance.

3.1.2. Nitric acid, nitrate and total nitrate

HNO_3 is evaluated at 8 EMEP stations located in eastern Europe, Nordic countries and Italy. Overall, CALIOPE-EU system is able to reproduce annual variability for HNO_3 (Fig. 3c), presenting the highest values during summer as measurements ($r = 0.41$, RMSE $= 1.1\ \mu g\ m^{-3}$). However, as shown also in Fig. 4c and d, CALIOPE-EU underestimates HNO_3 in coldest months (MFB $> -30\%$), has a small bias during spring (MFB $\leq \pm 30\%$, within the goals) and overestimates in summer (MFB $> 30\%$). CALIOPE-EU NO_2 concentrations have already been evaluated over EMEP in Pay et al. (2010a). The MFB for NO_2 was examined by season and did not show a strong seasonal trend, but the lowest bias are found in summer and spring (MFB $\sim -50\%$). This finding, together with an overestimation of HNO_3 in warm seasons indicates that either the chemical transport model (CMAQv4.5) may be generating too much nitric acid through photochemical reactions or summer deposition processes are not appropriately characterized (Baker and Scheff, 2007).

The NO_3^- concentrations are evaluated at 31 EMEP stations which cover mainly Spain and central Europe. Time series in Fig. 3d show that the modeling system reproduces the NO_3^- daily variability throughout the year ($r = 0.58$, RMSE $= 2.3\ \mu g\ m^{-3}$), presenting higher levels during winter and lower levels during summer due to its thermal instability (Querol et al., 2009). NO_3^- concentrations are on average underestimated, although large underestimations and errors are found in warm seasons (Fig. 4c and d) with |MFE| $\sim$ 130%. Note that summer underestimation occurs under low concentrations where relative model performance is not as important; indeed, both the model and observed NO_3^- are typically quite low during summertime (Fig. 3c). In any case, monthly fractional biases and errors for NO_3^- fall within the criteria. The NO_3^- errors are roughly 2 times higher than the corresponding SO_4^{2-} errors, reaching till 3 times in summer. Such finding is consistent with other modeling studies (Yu et al., 2005; Tesche et al., 2006). Diagnostic evaluations performed by Yu et al. (2005) indicate that a large source of error in simulating nitrate came from errors in the

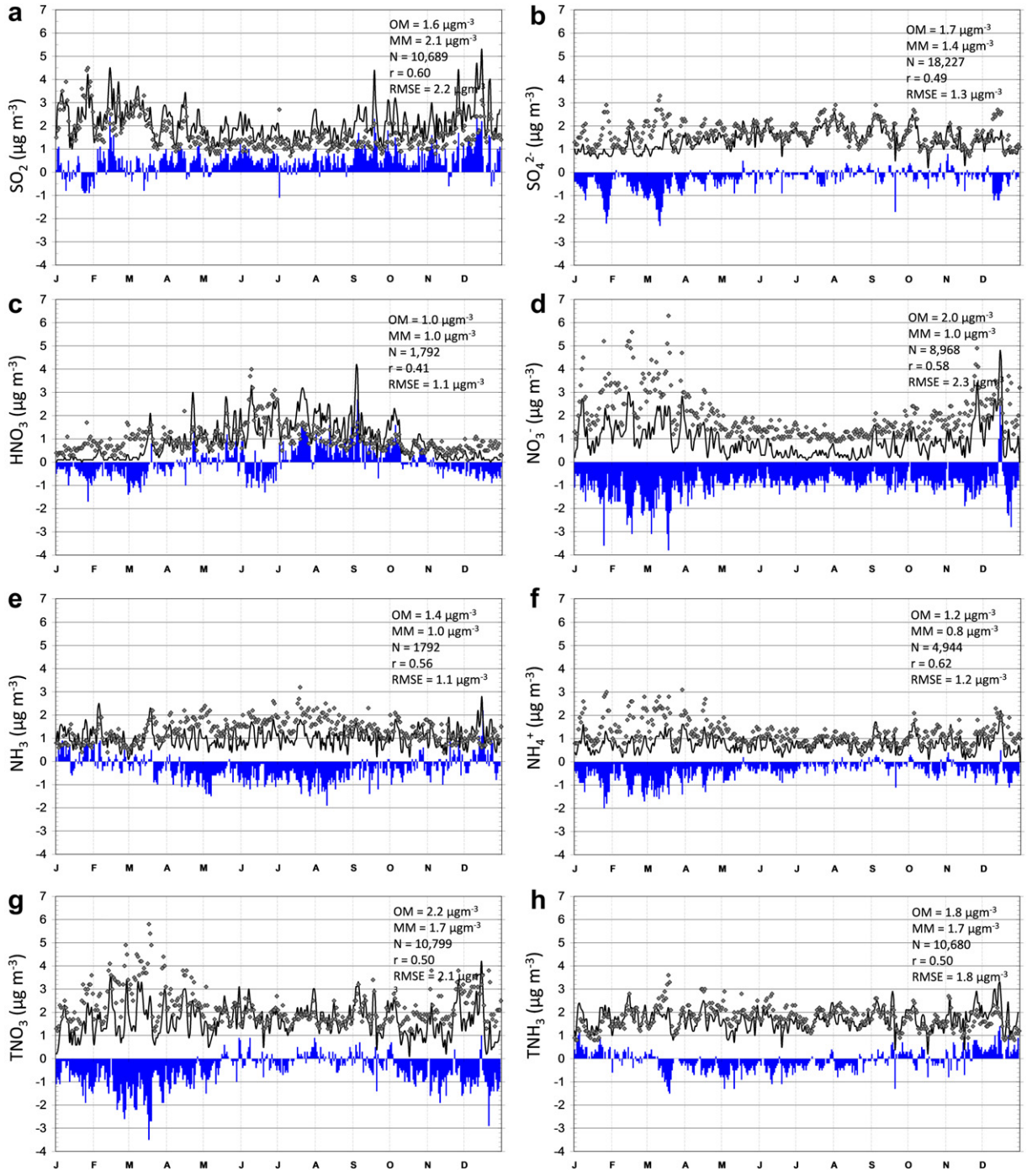

Fig. 3. Annual temporal series for SO_2 (a), SO_4^{2-} (b), HNO_3 (c), NO_3^- (d), gas-phase NH_3 (e), NH_4^+ (f), TNO_3 (g) and TNH_3 (h) on a daily basis calculated as an average over all EMEP stations in 2004. Diamonds represent EMEP measurements (in $\mu g\, m^{-3}$) and black continuous lines represent CALIOPE-EU outputs (in $\mu g\, m^{-3}$). Blue columns indicate daily mean bias ($\mu g\, m^{-3}$). Annual statistics are shown top-right: observed mean (OM), modeled mean (MM), number of data points (N), correlation coefficient (r) and root mean squared error (RMSE).

simulation of total ammonia, sulfate and, to lesser extent, total nitrate.

Measurements of TNO_3 are available at 31 stations covering Spain, north and central Europe. The TNO_3 in the modeling system reproduces the annual trend with high temporal correlation as shown the temporal series in Fig. 3g ($r = 0.50$, RMSE $= 1.1\ \mu g\, m^{-3}$). High modeled and measured levels of TNO_3 in winter can be explained by the higher stability of NH_4NO_3 in winter, which causes a higher portion of the NO_3^- to partition to aerosol, which has a longer lifetime than nitric acid against deposition (Schaap et al., 2004a). Monthly fractional biases and errors (Fig. 4c and d) indicate that large deviations are presented in the coldest months, dominated by the calculated underestimation of HNO_3 and NO_3^- in these seasons (MFB $< -50\%$). The low fractional bias in summer results from the compensation error between the overestimation of HNO_3 (MFB $\sim$ 50%) and underestimation of NO_3^- (MFB $\sim -130\%$). In warm months (from April to October) the fractional biases and errors are within the criteria: MFB $\leq \pm 60\%$ and MFE $\leq 75\%$.

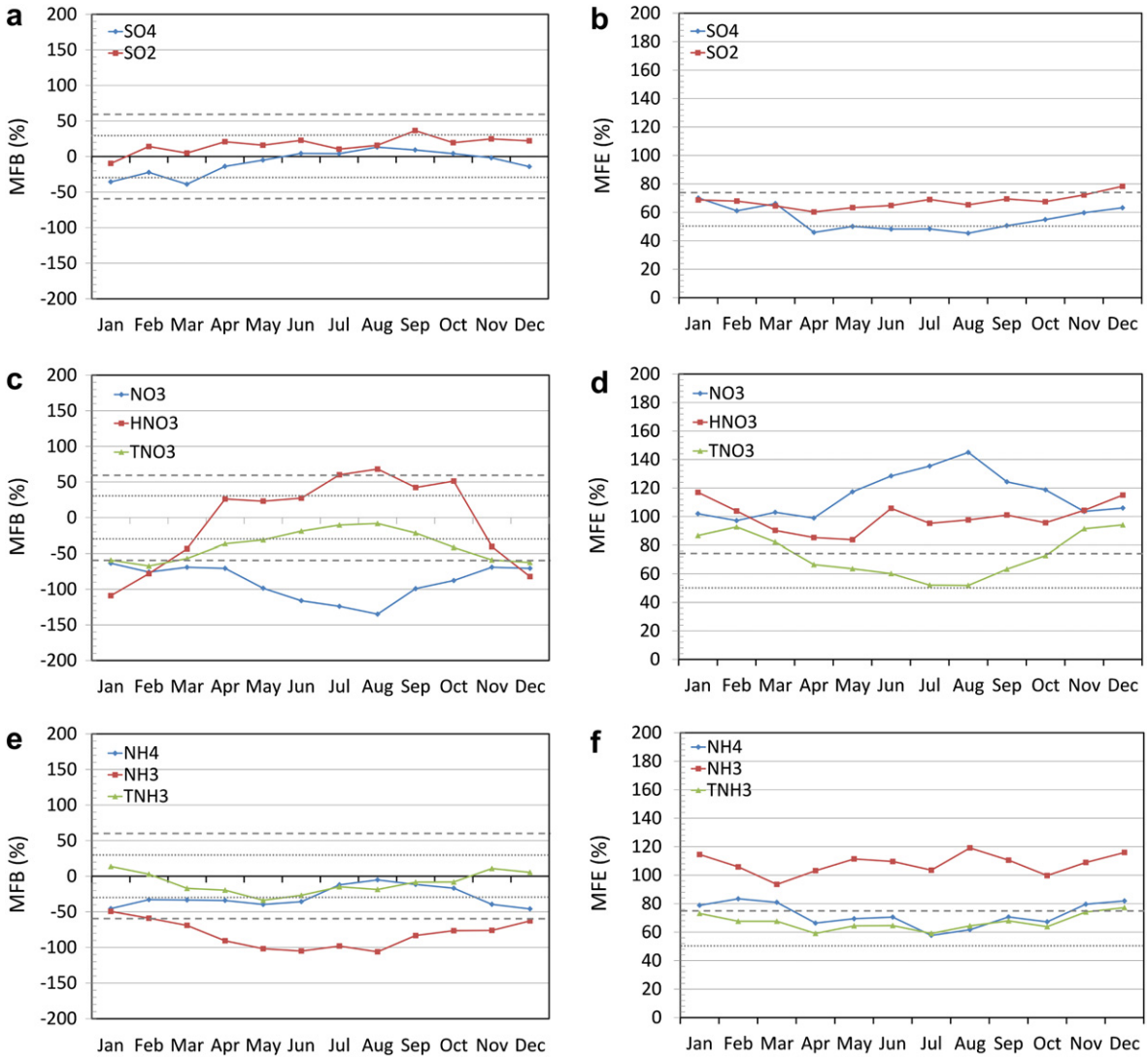

Fig. 4. Monthly Mean Fractional Bias (MFB, right column), and Mean Fractional Error (MFE, left column) compared with goals and criteria proposed by Boylan and Russell (2006). MFB and MFE are averaged over the sites within the EMEP network in 2004 for: SO_2 and SO_4^{2-} (a and b); HNO_3, NO_3^- and TNO_3 (c and d); and NH_3, NH_4^+ and TNH_3 (e and f). Dotted lines represent the goals (MFB $\leq \pm 30\%$ and MFE $\leq 50\%$). Broken lines represent the criteria (MFB $\leq \pm 60\%$ and MFE $\leq 75\%$).

The largest underestimations are located over the E.IP-W. Med and C. Med regions and the Eastern Europe (E. Eu regions, except Illmitz and Sniezka) with mean biases of $-1.8\ \mu g\ m^{-3}$ and $-1.5\ \mu g\ m^{-3}$, respectively in both areas. The model presents the best skills in the western Iberian Peninsula, with high correlations ranging from 0.40 to 0.65 by stations, and with annual mean biases less than $1.0\ \mu g\ m^{-3}$, and RMSE less than $1.3\ \mu g\ m^{-3}$.

3.1.3. Ammonia, ammonium and total ammonia

NH_3 is measured at 7 stations located in western Iberian Peninsula (2), central Mediterranean (1), and northern (2) and eastern (2) Europe. Temporal series (Fig. 3e) indicate that the CALIOPE-EU system reproduces the annual variability for NH_3 ($r = 0.56$) with a low mean bias (MB $= -0.4\ \mu g\ m^{-3}$) but significant normalized bias (30%). However, during warm season, April to August, modeled NH_3 is systematically underestimated. NH_3 emissions predominantly come from agricultural sources, primarily from livestock animal waste (Table 1). Livestock sources vary during the year since volatilization of NH_3 from the animal waste is a function of temperature (Gilliland et al., 2003). Seasonality in NH_3 emission is expected since field application of fertilizers occurs during specific seasons (Asman, 2001).

A total of 15 EMEP stations provide measurements of NH_4^+ to evaluate ammonium in 2004, mainly covering eastern Europe. Comparison of modeled NH_4^+ with measurement data (Fig. 3f) reveals that annual variability is correctly reproduced ($r = 0.62$, RMSE $= 1.2\ \mu g\ m^{-3}$). However, annual mean model is on average underestimated by 36%. Monthly fractional errors (Fig. 4e and f) fall within the criteria ($-60\% <$ MFB < 0 and MFE $< 75\%$) except in the coldest months. Despite the underestimations during winter, the temporal variability is correctly captured in these months ($r = 0.70$).

TNH_3 measurements are available at 31 stations covering Spain, north and central Europe. The temporal series (Fig. 3f) indicates that the TNH_3 levels are in general in agreement with observation along the year ($r = 0.50$, RMSE $= 2.1\ \mu g\ m^{-3}$) with relatively low bias (MB $= -0.5\ \mu g\ m^{-3}$). The fractional bias distribution by months (Fig. 4e and f) for TNH_3 shows that the modeling system does not provided enough TNH_3 in spring (MFB $\sim -25\%$) and lightly too much in winter (MFB $\sim$ 10%). TNH_3 falls within criteria for fractional bias and error, but partition between gas and aerosol is not totally well characterized. On one hand, TNH_3 underestimation in the warm season is biased by gas-phase NH_3 which presents its largest underestimation from May to August with MFF $\sim -100\%$

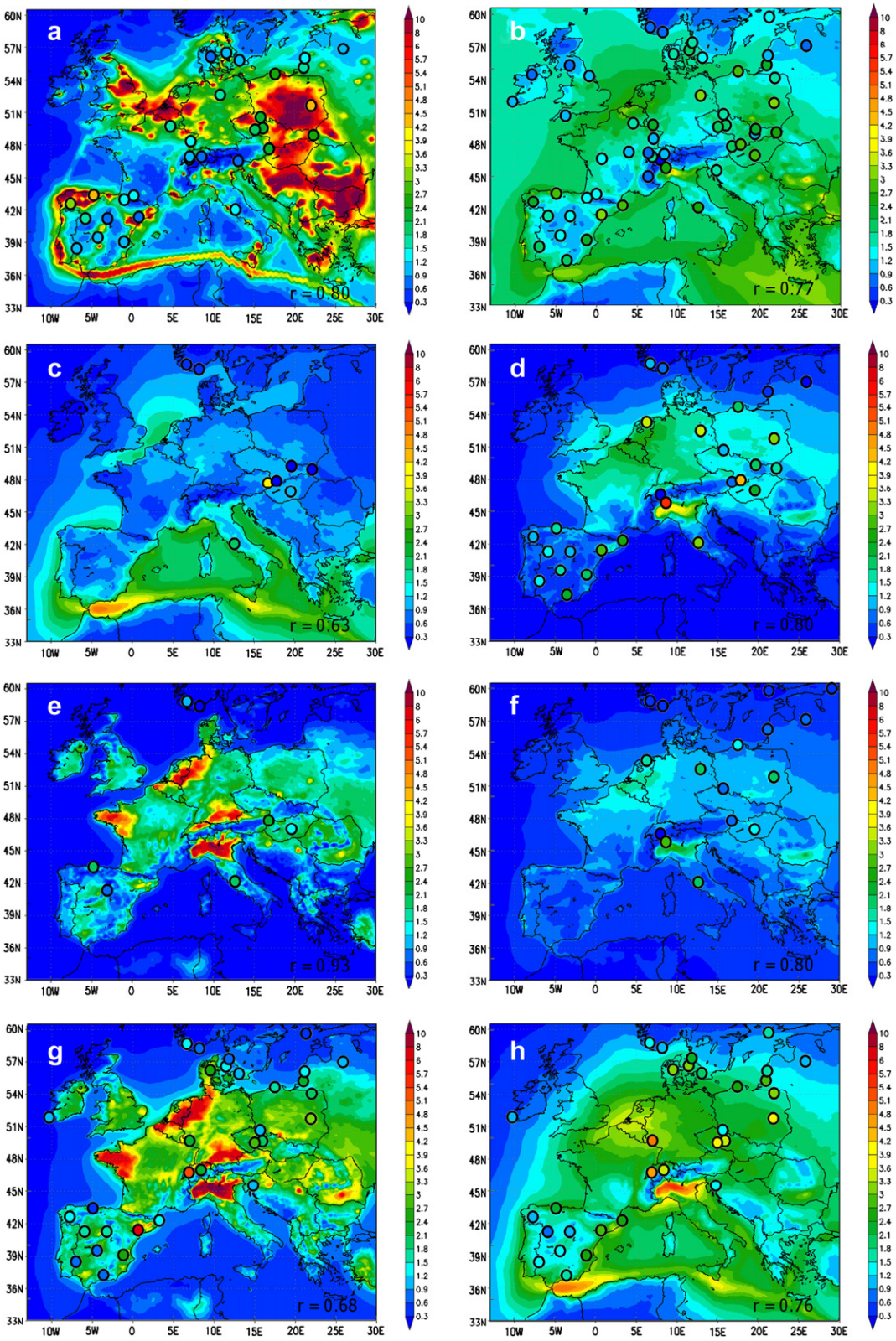

Fig. 5. 2004 annual mean distributions over Europe for SO_2 (a), SO_4^{2-} (b), HNO_3 (c), NO_3^- (d), gas-phase NH_3 (e), NH_3 (f), TNH_3 (g) and TNO_3 (h) at the lowest level. Points represent measured annual concentrations at the EMEP stations. Number at bottom-right in each figure is the spatial correlation between modeled and observed annual mean at each station.

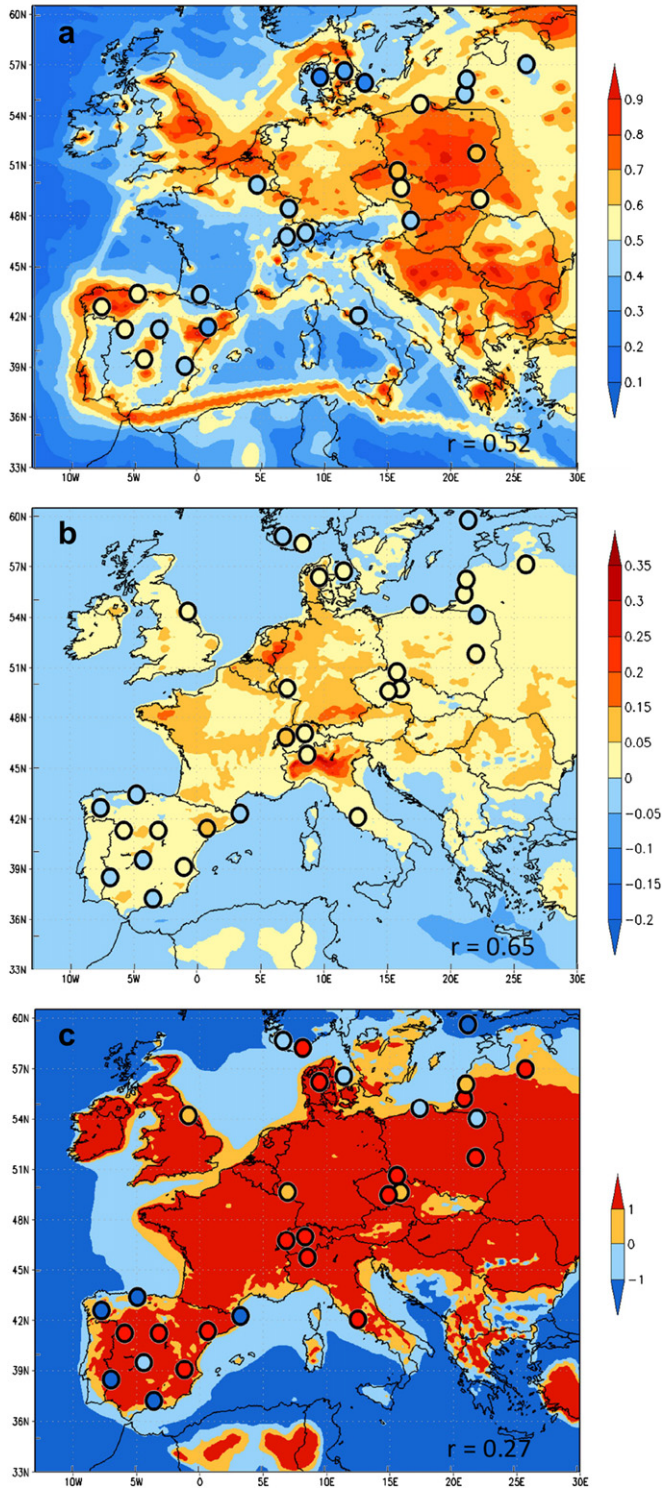

Fig. 6. Annual spatial distribution of the indicators: *S*-ratio (a), Free ammonia (b, in molar basin), and *G*-ratio (c) calculated within the CALIOPE-EU system over Europe in 2004. Dots represent the estimated indicators based on EMEP measurements.

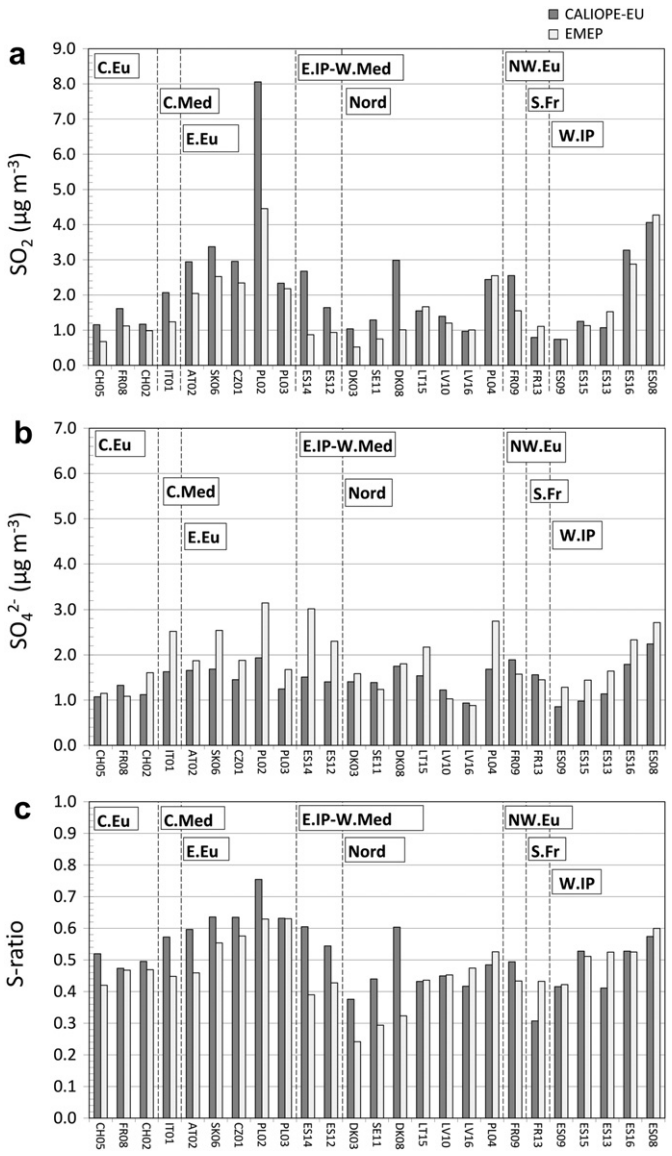

Fig. 7. Modeled and observed annual (a) SO_2 concentrations ($\mu g\,m^{-3}$), (b) SO_4^{2-} concentrations, and (c) *S*-ratio defined as $SO_2/(SO_2+SO_4^{2-})$ for each EMEP stations. The observed values are the light grey columns and the modeled values are the dark grey column. EMEP stations are represented by a code defined in Table 2 and they are sorted according to zones described in Table 2.

(Fig. 3e). On the other hand, TNH_3 overestimations in winter are biased by the tendency of the model to overestimate gas-phase NH_3 at some stations (Fig. 3e).

From May to October, SO_4^{2-} is overestimated (MFB ~10%) and NH_4^+ reaches its minimum bias (MFB ~ −10%). In this case, the underestimation of NH_3 during the same period suggests that the excessive SO_4^{2-} in the model keeps NH_4^+ in the particulate phase when it should be in the gas phase or available to potentially neutralize NO_3^-. This fact also explains the maximum overestimation of HNO_3 (MFB ~ 50%), the large underestimation of NO_3^- (MFB ~ −120%) and the minimum bias in TNO_3 (MFB ~ −20%) during the same period, since too much NO_3^- is remaining in the gas phase because there is not enough NH_4^+ to neutralized NO_3^-. This fact demonstrates that temporal representation of NH_3 emission could have a large effect on the results. Significant uncertainty exists in the magnitude and temporal variability of NH_3 emissions in Europe. In the CALIOPE-EU system, NH_3 annual emissions are temporal distributed applying fixed seasonal variations from the EMEP model (Fagerli and Aas, 2008). This methodology is widely used in chemical transport models such as CHIMERE (de Meij et al., 2009), TM5 (de Meij et al., 2006), MATCH (Langner et al., 2009). This methodology is simple because detailed agricultural registers

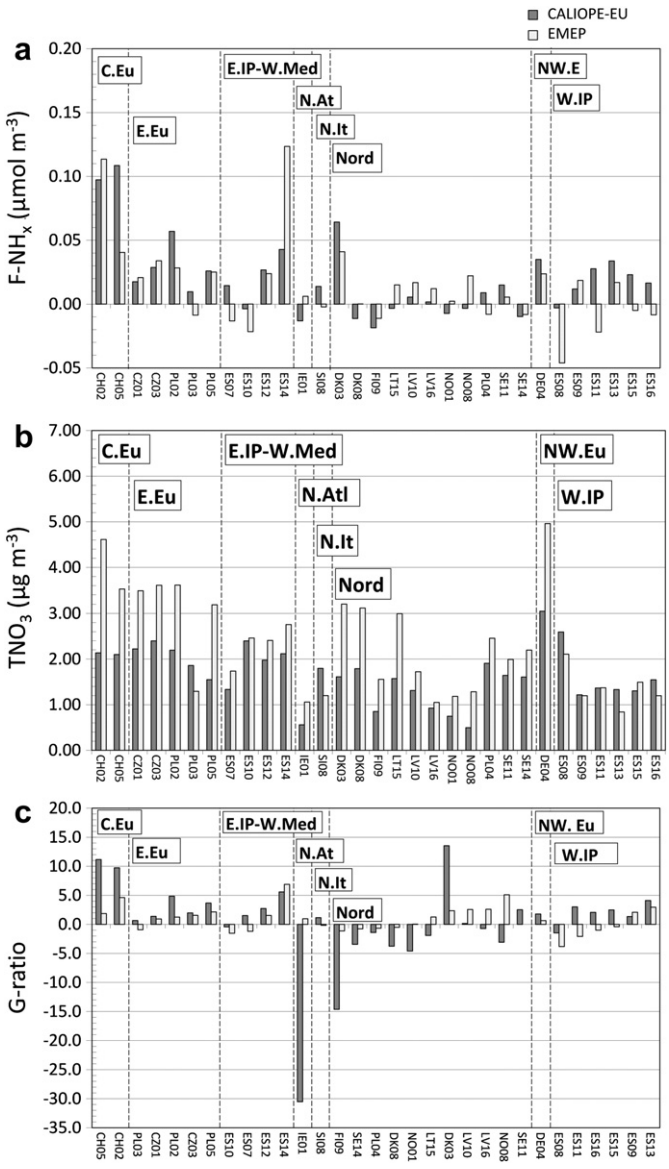

Fig. 8. Modeled and observed annual (a) Free ammonia (F-NH_x, μmol m^{-3}), (b) Total nitrate (TNO_3, μg m^{-3}), and (c) *G*-ratio defined as F-NH_x over TNO_3 on molar basis. The observed values are the light grey columns and the modeled values are the dark grey column. EMEP stations are represented by a code defined in Table 2 and they are sorted according to zones described in Table 2.

are not generally available in many countries. In the framework of COST ES0602, Menut and Bessagnet (2010) indicate that none of the 27 air pollution forecasting system, intercompared in the European domain, contains an accurate temporal profile for ammonia. The main limitation for such NH_3 emission model is the lack of reliable input data.

3.1.4. Bias relationship between SIA and gas precursors

The relationship in model-observation bias for SIA species and precursors is examined using the correlation coefficient (Table 3) to determine whether biases in gaseous precursors directly translate into biases for aerosol. These correlation coefficients compare the bias metric distributions at all sites and days for a pair of species. A number close to 1 indicates a strong relationship in the bias metric between a pair of species. A strong relationship is seen between model-observation bias for SO_4^{2-} and NH_4^+ (bias correlation = 0.59) and also between NO_3^- and NH_4^+ (bias correlation = 0.75). This makes sense since these ions are chemically coupled in the atmosphere. SO_2 bias has a fairly weak relationship with SO_4^{2-} bias, which is interesting since a more direct relationship might be expected between them. HNO_3 and NH_3 bias is weakly associated with biases in the aerosol species (bias correlation < 0.1). These weak relationships between biases in gaseous precursors and biases in aerosols indicate that model performance for precursors does not directly translate into model biases for SIAs in the same ambient sample. This likely reflects the different time scales of particulate formation and the influence of the regional transport.

3.2. Pattern description

Next section puts into words the simulated annual mean concentrations of SIA and their gas-phase precursors at ground level in 2004 combined with EMEP measurements.

3.2.1. Sulfur dioxide and sulfate

Fig. 5a shows model calculated SO_2 spatial distribution over Europe, which reflects the distribution of SO_2 emission sources in Fig. 1c. They are mainly produced by power generated and transformation industries (Table 1) located in northwestern Spain, eastern Europe, UK, Belgium and the southwestern Netherlands. These large point sources generate large plumes of high-SO_2 affecting the air quality on a local to regional scale. Background concentrations in eastern countries (8–20 μg m^{-3}) are greater than in West (~2 μg m^{-3}). Various large point sources of SO_2 in the east contribute to an increase of the regional concentration (30–50 μg m^{-3}). Over sea, the highest concentrations are found along the main shipping routes, since fuels used have high-SO_2 content. Modeled and measured annual means present high correlation at the 31 stations ($r = 0.80$), resulting from the detailed methodology of spatial disaggregation of EMEP inventory (50 km × 50 km) data over the high-resolution CALIOPE-EU grid (12 km × 12 km).

Concentration of SO_4^{2-} presents a spatial distribution more disperse than SO_2 due to SO_4^{2-} is partly produced during the transport of the SO_2 air masses (Fig. 5b). Regions with high levels of SO_4^{2-} correspond with important SO_2 emission point sources

Table 3
Correlation coefficients between CALIOPE-EU's biases for SIAs and gaseous precursors in 2004 at EMEP monitoring stations. Mean and standard deviation (STD) of the bias are in μg m^{-3}. Value reported without parenthesis represents the correlation coefficient. The first and second values in parenthesis represent the number of stations and the number of data points respectively used to calculate the correlation coefficient.

	NH_3	NO_3^-	HNO_3	SO_2	SO_4^{2-}	NH_4^+
Mean	−1.36	−1.01	−0.97	0.50	−0.29	−0.45
STD	1.09	2.10	1.64	2.14	1.31	1.08
NH_3	1.00 (7/2562)	0.03 (7/2562)	0.55 (5/1830)	−0.03 (4/1464)	0.02 (7/2562)	0.07 (5/1830)
NO_3^-		1.00 (27/9882)	−0.16 (8/2928)	−0.06 (15/5490)	0.29 (26/9516)	0.75 (14/5124)
HNO_3			1.00 (8/2928)	−0.07 (3/1098)	0.04 (8/2928)	0.00 (5/1830)
SO_2				1.00 (31/11346)	0.01 (25/9150)	0.07 (7/2562)
SO_4^{2-}					1.00 (53/19398)	0.59 (14/5124)
NH_4^+						1.00 (15/5490)

(Figs. 1c and 5a). The highest levels are found in eastern and south-eastern Europe and Po Valley (2–5 $\mu g\,m^{-3}$), followed by those obtained over the Benelux region and northeastern Spain (2–3 $\mu g\,m^{-3}$). The highest SO_4^{2-} levels over eastern Europe deplete the available gas-phase NH_3 so that little NH_4NO_3 can form due to the low NH_3 levels as can be seen latter in Fig. 5c. These findings are consistent with the results presented in Querol et al. (2009). In remote continental regions SO_4^{2-} mean levels range between 1 and 2 $\mu g\,m^{-3}$. However, over Scandinavia and elevated terrains (e.g. Alpine and Pyrenean chains) levels remain below 1.0 $\mu g\,m^{-3}$. The calculated spatial correlation at 53 EMEP stations indicates that there is a high agreement for background annual SO_4^{2-} concentration between model and observation over Europe, demonstrating that the CALIOPE-EU system is able to reproduce the main features of the intra-annual variability across Europe observed for SO_4^{2-}.

3.2.2. Nitric acid and nitrate

According to NO_2 performance, a detail discussion is provided in a separate paper Pay et al. (2010a). However, additional information about NO_2 is provided in the supplementary material. CALIOPE-EU is able to reproduce NO_2 distribution with good agreement over Europe, with spatial correlation of 0.75 (Fig. S1, supplementary material). Nevertheless, NO_2 background levels are significantly underestimated, MB = −3.7 $\mu g\,m^{-3}$ (Pay et al., 2010a).

The annual pattern of HNO_3 over Europe presents a high spatial variability (Fig. 5c). At continental regions the annual concentrations remain mainly below 1.0 $\mu g\,m^{-3}$, meanwhile over the sea concentrations are larger than those over land. Along the ship routes, where large amount of NO_x are emitted (Fig. 1c), the largest concentrations of HNO_3 are also modeled. Mean values in the Mediterranean Sea are ~ 3 $\mu g\,m^{-3}$ reaching maximum levels over the Alboran Sea along the Strait of Gibraltar (~5 $\mu g\,m^{-3}$), meanwhile over North Sea and English Channel HNO_3 levels are lower (~3 $\mu g\,m^{-3}$). The spatial correlation between modeled and measured annual means at 8 stations is 0.63 which is biased by the station of Illmitz where measurements seem to have more variability during winter than modeled (without Illmitz, the spatial correlation increase to 0.77).

NO_3^- spatial variability is high over Europe (Fig. 5d) with no clear relationship either anthropogenic activities or gas precursor HNO_3 (Fig. 5c) and NO_2 (Fig. S1, supplementary material). NO_3^- levels are significant over land, since NO_3^- concentrations rapidly decrease from the coast to open ocean. NO_3^- presents the highest concentration in the Po valley (between 3 and 4 $\mu g\,m^{-3}$) where both large anthropogenic sources of NO_x and NH_3 from agriculture and industrial-related sources are located. Elevated concentrations are also identified over The Netherland, Belgium, eastern Germany and northern France (~ 2.4 $\mu g\,m^{-3}$) which are affected by high levels of NH_3. Overall, in southern Europe (latitude < 44°N) NO_3^- concentrations are lower, not exceeding 1.5 $\mu g\,m^{-3}$ and remaining below 0.6 $\mu g\,m^{-3}$ over the sea. Despite the high HNO_3 levels due to ship tracks over the Mediterranean Sea, NO_3^- concentrations remain low because NH_3 availability is limiting. The annual spatial correlation shows a high agreement between CALIOPE-EU and EMEP observations ($r = 0.80$). Such good spatial correlation, modeled background mean NO_3^- levels are some how underestimated ~ 1 $\mu g\,m^{-3}$ over most of the stations as shown in the evaluation section.

Modeled TNO_3 annual distribution is shown in Fig. 5h. In continental region, as for NO_3^-, the highest concentrations of TNO_3 are found over the Po valley (~5 $\mu g\,m^{-3}$). Over the sea, the highest values are found along the maritime traffic routes and the Strait of Gibraltar (~4 $\mu g\,m^{-3}$). The spatial correlation for TNO_3 ($r = 0.76$) indicates a good agreement between the CALIOEP-EU system and EMEP concentration.

3.2.3. Ammonia and ammonium

Fig. 5e shows annual European pattern of gas-phase NH_3. Due to the short atmospheric lifetime of NH_3, its concentration field strongly resembles its emission distribution, as shown in Fig. 1a, and maximum concentrations occur in the areas with the highest emissions. Outside the source areas the NH_3 concentration declines rapidly (<1 $\mu g\,m^{-3}$). Maximum concentrations are located in The Netherlands and Po valley (~8 $\mu g\,m^{-3}$), followed by southern Germany and western France (~5 $\mu g\,m^{-3}$). Significant high levels (2–4 $\mu g\,m^{-3}$) are also found over southwestern France, northeastern Spain, central Poland and southeastern Europe. Comparisons with annual mean observations show high spatial correlation ($r = 0.93$). Nevertheless, this correlation is not representative since only 7 stations are available.

In air masses with a continental signature aerosol NO_3^- and SO_4^{-2} are associated with NH_4^+. In this sense, NH_4^+ presents a gradient distribution pattern more similar to SO_4^{2-} and NO_3^- than to NH_3 since NH_4^+ neutralizes those anions (Fig. 5f). NH_4^+ concentrations are ~1 $\mu g\,m^{-3}$ over most of Europe and decrease near the coast. Like for NO_3^-, the highest NH_4^+ concentrations are detected over the Po Valley (2–3 $\mu g\,m^{-3}$). High concentrations of NH_4^+ are also found over the Benelux region and southwestern Europe with values going from 1–2 $\mu g\,m^{-3}$. Low concentrations of NH_4^+ (<1.2 $\mu g\,m^{-3}$) are found in southern Europe (<40°N), and they are mainly present as $(NH_4)_2SO_4$, meanwhile HNO_3 remains in the gas phase. The lowest concentrations are found over Nordic counties and high mountains ranges (<0.6 $\mu g\,m^{-3}$). Annual mean spatial correlation shows a high agreement between model and observations ($r = 0.80$).

TNH_4 annual distribution is also shown in Fig. 5g; the pattern is obviously dominated by gas-phase NH_3. Spatial correlation for total ammonia is 0.68, lower than for NH_3 and NH_4^+. More stations are used to compute the correlation coefficient for TNH_3, and this result is deviated by the stations of Payerne and ElsTorms. Without these two stations spatial correlation increase to 0.71.

3.3. Indicators for SIA formation regimes

3.3.1. S-ratio

The ability of the model to form fine-particle SO_4^{2-} is investigated by the use of the *S*-ratio indicator (Hass et al., 2003). Fig. 6a presents the annual *S*-ratio distribution over Europe in 2004 modeled with CALIOPE-EU and measured at EMEP stations. Fig. 7c shows the observed and calculated annual *S*-ratios at each EMEP station lumping by regions (described previously in Table 2 and Fig. 2) and compared with the model performance for SO_2 (Fig. 7a) and SO_4^{2-} (Fig. 7b).

The observed *S*-ratios range from 0.24 (Tange-DK03) to 0.63 (Sniezka-PL03), meanwhile the modeled *S*-ratios tend to basically overestimate the observed range due to different regimes dominated in diverse regions. The highest *S*-ratio (observed and modeled *S*-ratio > 0.5) are found in eastern Europe and western Iberian Peninsula which indicates that fresh sulfur dominates these regions (oxidation processes are limiting). In this case, CALIOPE-EU overestimates these ratios, which is consistent with the model overestimation of the highest SO_2 levels, especially in eastern Europe (Fig. 7a and Section 3.1.1). *S*-ratios between 0.4 and 0.5 (modeled and observed) are found over the Mediterranean Basin (C. Med and E. IP-W. Med), central, northwestern, and north Europe (C. Eu, NW. E. and Nor.) where sulfur is dominated by SO_4^{2-} generated during the long-range transport. In this regime, CALIOPE-EU tends to overestimate *S*-ratio, mainly dominated by the SO_4^{2-} underestimations, which depict deficiencies of the SO_4^{2-} parameterizations (e.g. limitation to the availability of aqueous phase oxidants such as H_2O_2 and ozone as shown in other European studies (Stern et al., 2008; Schaap et al., 2004a; Kim et al., 2011).

The lowest observed and modeled *S*-ratios (*S*-ratios < 0.35) are found in northern Europe, at the stations of DK03, DK08 and SE11. Thus, this region is affected by SO_4^{2-} from transport, since no large isolated point sources are located there (Fig. 1a) and is only affected by ship emissions. Under this regime, CALIOPE-EU overestimates these ratios at these three stations, since modeled SO_2 levels are largely overestimated (Fig. 7a). This could indicate that ship emission estimates in the EMEP inventory are too high over these areas as pointed out by Tarrasón et al. (2007).

The spatial correlation is relatively high ($r = 0.52$) since it is biased by the under- and overestimation of sulfur compounds in different regions. Nevertheless, the modeled *S*-ratio over Europe is consistent with the patterns discussed before for SO_2 and SO_4^{2-}. On one hand, the major shipping routes (from the North Sea, passing by the English Channel, through Portugal, Spain and northern Africa toward the Suez Canal) and power plants in eastern Europe (Poland, Serbia, Rumania, Bulgaria and Greece), northwestern Spain and northwestern Europe (UK, Belgium, The Netherlands) are responsible for fresh sulfur. On the other hand, central Europe and over the Mediterranean Basin are regions affected by the secondary SO_4^{2-} transported form the aforementioned emitted areas which is secondary formed favored by the meteorological pattern (Querol et al., 2009).

3.3.2. Free ammonia

The F-NH_x indicator is a useful tool to identify potential regions with high potential to generate NH_3NO_3, based on the fact that it will be formed if there is enough NH_3 available after the neutralization of the SO_4^2. Fig. 6b presents the modeled annual F-NH_x distribution over Europe in 2004. Fig. 8a shows the observed and calculated annual F-NH_x at each EMEP stations lumped by regions.

Observed F-NH_x is in a range of −0.05 to 0.13 μmol m^{-3} (Fig. 8a). Calculated spatial correlation is relatively high ($r = 0.65$). However, the CALIOPE-EU system presents a tendency to overestimate F-NH_x. Under this condition, NH_4NO_3 could be enhanced in the model. Nevertheless, the partition of the nitrogen species between the gas and aerosol is very sensitive to ambient conditions (temperature and relatively humidity) on the area.

Modeled F-NH_x decreases from the coastal areas to the ocean. The lowest (modeled and observed) free ammonia (F-NH_x < 0 μmol m^{-3}) is mainly confined to coastal stations where neutralization by sea salt take place (Athanasopoulou et al., 2008).

Regions with low potentiality to form NH_4NO_3 (0 μmol m^{-3} < F-NH_x < 0.02 μmol m^{-3}) are found in northern Europe and western Iberian Peninsula. In the first case, it is due to the low emissions of NH_3 (Figs. 1a and 5e, respectively). In the second case, despite there is enough NH_3 emission, the elevated *S*-ratio regime indicates that available NH_3 is partitioned to aerosol phase to neutralized SO_4^{2-}.

Regions with relatively high potentiality to form NH_4NO_3 (0.02 μmol m^{-3} < F-NH_x < 0.04 μmol m^{-3}) are eastern Iberian Peninsula and eastern Europe. In both cases, NH_3 emissions are high, ~ 100–250 Mg yr^{-1} and 250–450 Mg yr^{-1} over localized areas (Fig. 1a). CALIOPE-EU tends to underestimate F-NH_x over Iberian Peninsula since TNH_3 is underestimated.

The highest measured and observed F-NH_x (F-NH_x > 0.04 μmol m^{-3}) are found in central (south Germany and Po valley) and northwestern Europe (Benelux and eastern France) where the highest and extended NH_3 emissions (>1400 Mg yr^{-1}) together with meteorological conditions (low temperature and high relatively humidity) favored the partition of NO_3^- to aerosol phase. In this case, CALIOPE-EU tends to overestimate the highest F-NH_x since TNH_3 are overestimated in those areas.

3.3.3. G-ratio

Fig. 6c shows the annual distribution pattern of observed and calculated *G*-ratios over 2004. *G*-ratio is useful to analyze which reactant, NH_3 or HNO_3, limits the formation of NH_4NO_3 (Ansari and Pandis, 1998). Fig. 8c shows the observed and calculated annual *G*-ratio at each EMEP stations compared with the performance of F-NH_x (Fig. 8a) and TNO_3 (Fig. 8b).

The modeled and observed spatial distribution of *G*-ratio indicates that, based on annual average concentration, over continental Europe the NH_4NO_3 formation is limited by the formation of HNO_3 (*G*-ratio > 1). Adams et al. (1999) showed the same tendency over the European continent using the global model GISS GCM II. Also Sartelet et al. (2007) and Kim et al. (2011) estimated the same pattern over continental areas with the POLYPHEMUS system using different chemical mechanisms (CB05 and RACM). Such findings indicate that NH_4NO_3 concentration in these areas could increase dramatically given an increase in HNO_3 concentration, or indirectly given an increase of NO_x emissions. It is also consistent with results obtained by Renner and Wolke (2010) over northwestern Europe, who demonstrate that ammonium nitrate, but above all ammonium sulfate, is not sensitive to NH_3 emission changes when SO_2 and NO_x are limiting.

Over ocean, NO_3^- is produced over the English Channel, Atlantic coast of France, and the North Sea, although NH_3 limits its formation (0 < *G*-ratio < 1). An acidic sulfate aerosol dominates the Mediterranean Sea (*G*-ratio < 0) severely limited by NH_3, where intense maritime traffic generate high NO_x (indirectly HNO_3) and SO_2 emissions.

The low spatial correlation ($r = 0.27$) are related with the fact that this equation may be too simplistic for location where NO_3^- is often neutralized by sodium or calcium, such as coastal areas or western Mediterranean Basin (Athanasopoulou et al., 2008; Querol et al., 2009). The CALIOPE-EU system estimates sea-salt emissions from open oceans. In spite of this, the replacement of Cl^- by NO_3^- in mixed marine/urban air masses is not implemented in the AERO4 module of CMAQv4.5 (Kelly et al., 2010).

4. Comparison with other CTM evaluation studies

Recent CTM studies have provided more insight in the SIA formation in Europe. This section discusses a comparative analysis between various European model evaluations and the results obtained here from the CALIOPE-EU system. Note that this is not an exhaustive inter-comparison study because of the different configuration of the diverse works. Nevertheless, it provides a good basis for assessing the reliability of the results obtained in the context of the European model evaluation which also complement that presented in Pay et al. (2010a). Table 4 shows a chronological list of published CTM evaluation studies on SIA and precursors gases, which are presented along with CALIOPE-EU evaluation results. Following the criteria in Pay et al. (2010a) those evaluation studies have several characteristics in common: (1) European domain; (2) the regional scale (horizontal resolutions are from 12 km to 55 km); (3) the simulation period, mainly annual, except in the case of Kim et al. (2011) and Stern et al. (2008); and (4) the used of the EMEP monitoring network to evaluate the models. Table 5 presents the common statistics for the fine inorganic aerosols (SO_4^{2-}, NO_3^- and NH_4^+). Gas-phase aerosol precursors (nitric acid and ammonia) and total nitrate and ammonia are presented in Table 6. Results for sulfur dioxide are presented at Table 5 in Pay et al. (2010a). Three common statistics parameters are considered: Ratio, *r*, and RMSE.

For SO_4^{2-} concentration CALIOPE-EU presents satisfactory annual correlations in comparison to the other studies (0.49 versus 0.37–0.65 in annual basis). However, the RMSE obtained with CALIOPE-EU is the lowest form all the models (1.3 μg m^{-3} for CALIOPE-EU versus 1.7–5.89 μg m^{-3}). As other European modeling system, CALIOPE-EU tends to underestimate SO_4^{2-} annual concentrations.

Table 4
List of published European model evaluation studies for secondary inorganic aerosols and their main characteristics to be compared with CALIOPE-EU evaluation results (this study).

Reference	Modeled year[a]	Modeling system	Horizontal resolution/layers	Chemical mechanism[b]	Thermodynamic inorganic equilibrium[c]	Study number
This study	2004	CALIOPE	12 km × 12 km/15	CBM-IV	ISORROPIA	CALIOPE-EU04
Kim et al. (2011)	2001	POLYPHEMUS	0.5° × 0.5°/5	RACM	ISORROPIA	POLYPHEMUS1
Kim et al. (2011)	2001	POLYPHEMUS	0.5° × 0.5°/5	CB05	ISORROPIA	POLYPHEMUS2
Matthias (2008)	2001	CMAQ	54 km × 54 km/20	CBM-IV	ISORROPIA	CMAQ3
Stern et al. (2008)	2003	CHIMERE	0.25° × 0.25°/8	MELCHIOR	ISORROPIA	CHIMERE4
Stern et al. (2008)	2003	EURAD	125 km × 125 km/23	EuroRADM	RPMARES	EURAD4
Stern et al. (2008)	2003	LOTOS-EUROS	0.25° × 0.25°/4	CBM-IV	ISORROPIA	LOTOS-EUROS4
Stern et al. (2008)	2003	REM-CALGRID	0.25° × 0.25°/5	CBM-IV	ISORROPIA	REM-CALGRID4
Stern et al. (2008)	2003	LM-MUSCAT	0.25° × 0.25°/40	RACM	Hinneburg et al. (2007)	LM-MUSCAT4
Sartelet et al. (2007)	2001	POLYPHEMUS	0.5° × 0.5°/5	RACM	ISORROPIA	POLYPHEMUS5
Tarrasón et al. (2006)	2004	Unified EMEP	50 km × 50 km/20	EMEP	EQSAM	EMEP6
van Loon et al. (2004)	1999/2001	CHIMERE	0.5° × 0.5°/8	MELCHIOR	ISORROPIA	CHIMERE7
van Loon et al. (2004)	1999/2001	DEHM	50 km × 50 km/20	EMEP	EQSAM	DEHM7
van Loon et al. (2004)	1999/2001	Unified EMEP	50 km × 50 km/10	EMEP	EQSAM	EMEP7
van Loon et al. (2004)	1999/2001	MATCH	55 km × 55 km/10	EMEP	EQSAM	MATCH7
van Loon et al. (2004)	1999/2001	LOTOS	0.25° × 0.5°/3	CBM-IV	ISORROPIA	LOTOS7
van Loon et al. (2004)	1999/2001	CMAQ	36 km × 36 km/21	RADM2	ISORROPIA	CMAQ7
van Loon et al. (2004)	1999/2001	REM-CALGRID	0.25° × 0.5°	CBM-IV	ISORROPIA	REM-CALGRID7
Schaap et al. (2004a,b)	1995	LOTOS	25 km × 25 km/3	CBM-IV	ISORROPIA	LOTOS8
Hass et al. (2003)	1995	DEHM	50 km × 50 km/10	CBM-IV	EQSAM	DEHM9
Hass et al. (2003)	1995	EURAD	27 km × 27 km/15	EuroRADM	RPMARES	EURAD9
Hass et al. (2003)	1995	EUROS	0.55° × 0.55°/4	CBM-IV	EQSAM	EUROS9
Hass et al. (2003)	1995	LOTOS	0.25° × 0.5°/3	CBM-IV	ISORROPIA	LOTOS9
Hass et al. (2003)	1995	MATCH	55 km × 55 km/10	EMEP	EQSAM	MATCH9
Hass et al. (2003)	1995	REM-CALGRID	0.25° × 0.5°	CBM-IV	ISORROPIA	REM-CALGRID9

[a] Evaluation studies are done over a full year. Evaluated period for Kim et al. (2011) corresponds from 15 July to 15 August. Evaluated period for Stern et al. (2008) corresponds from 6 February to 30 March.
[b] CB-IV, see Gery et al. (1989); CB05, see Yarwood et al. (2005); EMEP, see Simpson et al. (2003); EuroRADM, see Stockwell and Kley (1994); MELCHIOR, see Schmidt et al. (2001); RACM, see Stockwell et al. (1997); RADM2, see Stockwell et al. (1990).
[c] ISORROPIA, see Nenes et al. (1998); RPMARES, see Binkowski and Shankar (1995); EQSAM, see (Metzger et al., 2002).

Table 5
Comparison of the following statistics: modeled mean/observed mean (Ratio), correlation coefficient (r), and root mean squared error (RMSE, $\mu g\ m^{-3}$) on a daily basis between CALIOPE-EU and other European models[a, b] for secondary inorganic aerosols (SO_4^{2-}, NO_3^-, and NH_4^+).

Study number	SO_4^{2-} daily average			NO_3^- daily average			NH_4^+ daily average		
	Ratio	r	RMSE	Ratio	r	RMSE	Ratio	r	RMSE
CALIOPE-EU04	0.82 (0.56, 2.0)	0.49 (0.15, 0.81)	1.30 (0.3, 2.3)	0.50 (0.14, 2.0)	0.58 (0.20, 0.77)	2.30 (0.6, 3.8)	0.67 (0.38, 1.35)	0.62 (0.30, 0.73)	1.20 (0.3, 4.1)
POLYPHEMUS1	0.86			1.5			1.1		
POLYPHEMUS2	0.96			1.7			1.2		
CMAQ3	0.83 (0.54, 1.36)	(0.21, 0.72)		0.62 (0.39, 1.0)	(0.30, 0.80)		0.75 (0.53, 0.94)	(0.30, 0.75)	
CHIMERE4	0.69	0.48	3.4						
EURAD4	0.64	0.46	3.3						
LOTOS-EUROS4	0.57	0.47	3.7						
REM-CALGRID4	0.99	0.47	2.9						
LM-MUSCAT4	0.91	0.57	2.7						
POLYPHEMUS5	0.84	0.56	1.7	1.6	0.41	3.1	1.1	0.52	1.3
EMEP6	0.86	0.67		1.4	0.80		1.2	0.82	
CHIMERE7	0.67/0.72	0.49/0.53	2.5/2.07	0.94/0.80	0.44/0.46	2.74/2.73	1.11/1.01	0.41/0.56	1.27/1.38
DEHM7	0.93/0.85	0.57/0.55	2.36/1.77	1.80/1.63	0.34/0.25	3.02/2.53	1.10/0.79	0.51/0.49	0.98/0.83
EMEP7	0.91/0.88	0.57/0.58	2.1/1.84	1.63/1.04	0.50/0.34	3.51/2.08	1.26/1.00	0.51/0.47	1.22/0.86
MATCH7	1.0/1.17	0.56/0.62	2.1/1.86	0.88/0.83	0.47/0.40	1.74/1.59	1.01/1.62	0.53/0.55	0.94/2.09
LOTOS7	1.03/1.3	0.37/0.50	2.9/2.89	0.79/0.95	0.26/0.17	2.19/1.94	1.21/1.01	0.37/0.44	1.21/1.10
CMAQ7	1.22/–	0.46/–	2.67/–	2.65/–	0.47/–	1.74/–	–/–	–/–	–/–
REM-CALGRID7	0.91/0.93	0.51/0.53	2.36/2.03	1.15/0.74	0.42/0.35	2.43/1.92	1.33/1.23	0.45/0.45	1.24/0.99
LOTOS8	0.92	0.60	2.60	1.10	0.58	3.57	1.08	0.62	1.54
DEHM9	1.11	0.37	5.89	1.07	0.32	4.12	0.94	0.39	2.43
EURAD9	1.52	0.52	4.25	2.04	0.61	6.14	1.87	0.50	2.90
EUROS9	0.98	0.47	4.39	2.13	0.30	6.39	–	–	–
LOTOS9	0.91	0.54	2.76	1.59	0.49	4.07	1.23	0.51	1.57
MATCH9	0.84	0.65	2.49	0.78	0.50	2.55	0.55	0.61	1.46
REM-CALGRID9	0.81	0.50	2.78	1.07	0.53	3.10	1.07	0.43	1.63

[a] Value reported without parenthesis represents yearly averages in the entire domain. The first and second values in parenthesis represent the minimum and maximum value respectively obtained among all stations in the entire domain.
[b] Values reported with a slash correspond to two different years studied: the number before the slash corresponds to the year 1999; the number after the slash correspond to the year 2001.

Table 6
Comparison of the statistics modeled mean/observed mean (Ratio), correlation coefficient (r), and root mean squared error (RMSE, $\mu g\,m^{-3}$) between CALIOPE-EU and other European models[a, b] for total nitrate ($TNO_3 = HNO_3 + NO_3^-$), total ammonia ($TNH_3 = NH_3 + NH_4^+$) and gas-phase aerosol precursors (HNO_3 and NH_3) in daily basis. Note that the other gas-phase aerosol precursors, SO_2 and NO_2 have been compared with other European studies in Pay et al. (2010a).

Study number	HNO_3 daily average			TNO_3 daily average			NH_3 daily average			TNH_3 daily average		
	Ratio	r	RMSE	Ratio	r	RMSE	Ratio	r	RMSE	Ratio	r	RMSE
CALIOPE-EU04	1.00 (0.35, 4.0)	0.41 (−0.11, 0.78)	1.1 (0.4, 3.5)	0.77 (0.45, 1.2)	0.50 (0.14, 0.70)	2.1 (0.9, 3.6)	0.71 (0.1, 1.0)	0.56 (0.10, 0.40)	1.1 (0.3, 1.3)	0.94 (0.62, 2)	0.50 (0.10, 0.72)	1.8 (0.4, 3.3)
CHIMERE4				0.70	0.47	4.4				1.1	0.49	1.9
EURAD4				2.90	0.46	19.4				3.0	0.45	8.3
LOTOS-EUROS4				0.94	0.67	3.1				1.0	0.58	1.6
REM-CALGRID4				0.87	0.56	3.5				1.4	0.57	2.1
LM-MUSCAT4				0.44	0.42	5.8				1.6	0.56	3.5
POLYPHEMUS5	1.85	0.26	1.4				0.85	0.29	5.4			
EMEP6	0.73	0.38		1.23	0.87					1.26	0.63	
CHIMERE7				0.90/0.83	0.39/0.37	3.02/2.82				1.18/1.05	0.35/0.43	2.98/1.74
DEHM7				1.68/1.73	0.42/0.31	3.03/3.02				0.86/0.79	0.46/0.45	1.85/1.14
EMEP7				1.40/1.16	0.51/0.36	2.62/2.42				1.05/1.00	0.42/0.40	1.95/1.28
MATCH7				0.85/0.95	0.52/0.41	1.88/1.91				0.71/1.62	0.48/0.42	1.82/2.17
LOTOS7				0.72/0.70	0.23/0.20	2.31/2.27				1.12/1.01	0.27/0.29	2.25/1.49
CMAQ7				1.82/–	0.52/–	1.88/–				–/–	–/–	–/–
REM-CALGRID7				1.10/0.86	0.39/0.31	2.26/3.02				1.35/1.23	0.27/0.30	2.39/1.49
LOTOS8				0.81	0.52	2.31				0.88	0.58	1.50
DEHM9				1.09	0.45	2.75	0.38	0.27	7.38	0.79	0.47	3.69
EURAD9				1.85	0.50	3.72	0.56	0.15	5.88	1.24	0.54	3.40
EUROS9				2.49	0.41	5.17	–	–	–	–	–	–
LOTOS9				1.67	0.44	2.82	0.18	0.05	7.50	0.58	0.46	2.77
MATCH9				0.94	0.52	1.94	0.64	0.33	5.59	0.84	0.57	2.54
REM-CALGRID9				1.20	0.38	2.13	0.58	0.09	6.10	0.91	0.26	3.09

[a] Value reported without parenthesis represents yearly averages in the entire domain. The first and second values in parenthesis represent the minimum and maximum value respectively obtained among all stations in the entire domain.
[b] Values reported with a slash correspond to two different years studied: the number before the slash corresponds to the year 1999; the number after the slash correspond to the year 2001.

Considering NO_3^-, the annual correlation obtained for CALIOPE-EU ($r = 0.58$) is, with LOTOS8, the third highest value after EURAD9 ($r = 0.61$) and the EMEP6 ($r = 0.80$). Note that EMEP6 presented also the highest correlation for NO_2 (Pay et al., 2010a). The other studies calculated lower correlations for nitrate ranging from 0.17 to 0.50. The RMSE for CALIOPE-EU are in a lower range than the other studies (2.30 $\mu g\,m^{-3}$ against 1.59–6.39 $\mu g\,m^{-3}$). Differently from the other European modeling system, CALIOPE-EU tends to simulates slightly lower aerosol nitrate concentrations than those measured presenting the lowest Ratio (Ratio = 0.50), closely followed by CMAQ3 (Ratio = 0.63).

As for NO_3^-, the annual correlation for NH_4^+ obtained within CALIOPE-EU ($r = 0.62$) is the same as for LOTOS8, and the second highest value after EMEP6 ($r = 0.82$). The other studies present lower correlations but always higher than those obtained for NO_3^- (0.39–0.61). RMSE for CALIOPE-EU is in the same range as the other studies (1.20 $\mu g\,m^{-3}$ against 0.83–2.90 $\mu g\,m^{-3}$). Again, conversely from the other studies, CALIOPE-EU tends to underestimate NH_4^+, presenting the second lowest Ratio (Ratio = 0.67), after MATCH9 (Ratio = 0.55) and relatively closer to CMAQ3 (Ratio = 0.75).

As discussed in Pay et al. (2010a), the CALIOPE-EU evaluation results for SO_2 show very satisfactory performances in comparison with other studies, mainly attributed to the high resolution of the CALIOPE-EU system which enables a well-defined allocation of SO_2 sources over Europe. As CALIOPE-EU most of the European models present the a tendency to overestimate SO_2, e.g. bias of 1.3 $\mu g\,m^{-3}$ for CALIOPE-EU versus biases between 1.0 and 2.3 $\mu g\,m^{-3}$ for EUROTRAC models (Hass et al., 2003). For HNO_3, not too much comparison can be done since there are only few stations that measured this compound. Annual correlation coefficient is higher than that presented in other studies (0.41 for CALIOPE-EU versus 0.26 (POLYPHEMUS5) − 0.38 (EMEP6)). RMSE is in the same range than that obtained POLYPHEMUS5.

Overall, CALIOPE-EU performances for NH_3 are superior to other European studies. The correlation obtained is this study is the highest from all considered models (0.56 against 0.05–0.33). The RMSE is in the lowest range from other European studies (1.1 $\mu g\,m^{-3}$ for CALIOPE-EU versus 5.40–7.50 $\mu g\,m^{-3}$). As other European studies, the CALIOPE-EU system tends to underestimate NH_3 in the gasphase (0.77 against 0.18–0.85). Given the strong gradients in NH_3 levels, the high resolution of CALIOPE-EU, both vertical and horizontal, could justify its better skills to reproduce the large NH_3 gradients compared to other European models (Asman, 2001).

For TNO_3, correlations are in the same range of the other European studies (0.50 for CALIOPE-EU against 0.37–0.56). Only EMEP6 is out the mean ($r = 0.87$) consistently with its highest correlation for NO_3^-. RMSE for all the models is in the same range (2.1 for CALIOPE-EU versus 1.80 $\mu g\,m^{-3}$–3.70 $\mu g\,m^{-3}$). Similar results for TNO_3 are found in LOTOS8 for correlation (0.50 against 0.52), RMSE (2.1 $\mu g\,m^{-3}$ against 2.3 $\mu g\,m^{-3}$), and a similar tendency to underestimate TNO_3 (Ratio = 0.77 vs. Ratio = 0.81). As for TNO_3, statistics for TNH_3 modeled by the CALIOPE-EU system is in the range of other studies.

The different performance of SIAs and gaseous precursors seems to be related with the chemical mechanism and thermodynamic equilibrium. Most of European models in this comparison used the CB-IV chemical mechanism. The CB-IV has recently been updated, namely CB05 (Yarwood et al., 2005). Yu et al. (2010) found that CB05 has the relatively better performance for HNO_3 and SO_2 than for CB-IV. This update is interesting since, as showed before, NO_3^- formation tends to be HNO_3-limited over continental areas. Recently, Kim et al. (2011) tested the impact of RACM2 (updated version of RACM) and CB05 on the formation of SIA over Europe and showed that differences in SIA result from differences in oxidant concentration (OH, O_3 and NO_3).

According to the thermodynamic equilibrium, EQSAM module (Metzger et al., 2002) is widely used in EMEP model and global models (MATCH and DEHM). This module is very simplified and tends to partition too much NO_3^- and NH_4^+ to aerosol phase under lower temperatures (Tarrasón et al., 2006) causing the aforementioned overestimation of these species. ISORROPIA has

proved to be the model of choice for many three-dimensional air quality models in Europe due to its computational efficiency and rigor. Both EQSAM and indeed ISORROPIA tend to predict too stable ammonium nitrate in winter and at night, whereas in summer and at day-time calculated aerosols are too unstable. Results in Schaap et al. (2010) indicate that the equilibrium assumption is not valid and/or that the ISORROPIA module is not able to describe partitioning correctly under conditions encountered in the Netherlands. Another important limitation of ISORROPIA is the lack of treatment of crustal species (Ca, K, Mg), important in simulating the partitioning of NO_3^- and NH_4^+, especially in areas like the southern Europe where dust (from deserts or resuspended form arid areas) comprise a significant portion of PM10 and PM2.5 (Querol et al., 2009). Recently, an update version of ISORROPIA that includes crustal species has been published, namely ISORROPIA II (Fountoukis and Nenes, 2007).

5. Summary and conclusions

This paper presents the evaluation results of the CALIOPE-EU system in terms of SIAs and their gaseous precursors using a full-year simulation for 2004 over Europe and its use for assess SIA formation regimes over Europe. Modeled results have been compared to long-term surface concentrations from the EMEP monitoring network and to other European evaluation studies. The evaluation is focused on the capability of the model to reproduce (1) the temporal and spatial distribution of SIAs and their precursors, in terms of statistics; and (2) the inorganic aerosol formation regimes, in terms of so-called indicators.

Calculated spatial correlation coefficients between model and measurements indicate that CALIOPE-EU is able to reproduce SIA concentrations across Europe with coefficients ranging from 0.76 to 0.80. Although the total amount of SIAs is on average underestimated by 18–50% in most regions of Europe, the temporal variability and hence the transport patterns of these species are captured rather well, as indicated by the correlation coefficients, which range between 0.49 and 0.62. Based on fractional biases and errors, the CALIOPE-EU's performance for HNO_3 and NH_3 gaseous precursors is not as accurate as for NO_3^- and NH_4^+ aerosols.

Although the concentrations of SIAs are on average underestimated by 18–50% in most regions of Europe, their temporal variability are captured rather well, as indicated by the correlation coefficients, which range from 0.49 till 0.62. SO_2 is systematically overpredicted by the CALIOPE-EU system which suggests that SO_4^{2-} formation in the modeling system is often limited by oxidant availability and not always by SO_2. Overall NO_3^- concentrations are underestimated in -60% in winter and $<-100\%$ in summer. The CALIOPE-EU system does not estimate the formation of coarse NO_3^- through reaction of HNO_3 with sea salt or dust. On the other hand, the uncertainty of NO_3^- and HNO_3 measurements hampers to discern if the model overestimation of HNO_3, especially in summer, results from deficiency in model-process description. The summer overestimation of HNO_3 and underestimation of NO_3^- could have minimal impact on regulatory applications since the warm temperatures do not favor the ammonium nitrate formation.

Simulated NH_4^+ concentrations were generally underestimated ($\sim$ 20%). Two factors that most strongly influence simulated NH_4^+ concentration in Europe are NH_3 emissions and SO_4^{2-} concentration. Modeled NH_3 does not compare with observation as well as NH_4^+ does. The modeled NH_3 concentrations are underestimated by $\sim$100% during summer.

SIAs and their gas precursors have been also analyzed in terms of goals and criteria following Boylan and Russell (2006). SO_2/SO_4^{2-} and TNH_3/NH_4^+ monthly concentrations accomplish the criteria for bias and errors. TNO_3 falls within the criteria in warm seasons for biases and errors. The larger errors and fraction biases are found for HNO_3 and NO_3^-.

That evaluation experience also demonstrates that there is a weaker relationship between biases in SIAs and their gaseous precursors than between SIAs each other. This reflects the different time scale of particulate formation and the influence of the regional transport.

Concerning spatial evaluation, correlation coefficients between model and measurements indicate that CALIOPE-EU is able to reproduce SIA concentrations across Europe with coefficients ranging from 0.76 to 0.80. SO_4^{2-} presents a clear west-east gradient over Mediterranean Basin, dominated by the large isolated sources located in eastern Europe. In contrast with SO_4^{2-}, NO_3^- presents a prominent east–west and south–north increasing gradient over Europe. Special features may account for these differences: (1) the high levels of SO_4^{2-} in eastern Europe depletes the available gas-phase NH_3 so that little NH_4NO_3 can form in this region due to the low NH_3 levels; (2) the higher ambient temperature in the south favors the gas phase prevalence of NO_3^-; and (3) the high humidity conditions in the north which stabilize NH_4NO_3 even during the summer. Despite the high HNO_3 levels due to ship tracks over the Mediterranean Sea, NO_3^- concentrations remain low because NH_3 availability is limiting. Gas-phase NH_3 concentrations are high in continental areas with high NH_3 emissions, particularly if little SO_4^- is present. NH_3 concentrations are found to be highest regionally in UK, The Netherlands, southwestern France, Po valley, central Poland, southeastern Europe and southern Sweden.

The comparison with previous modeling results indicate that the CALIOPE-EU's evaluation with EMEP measurements presents high scores for SO_4^{2-}, and gaseous precursors (SO_2, HNO_3 and NH_3). Most models are based on EMEP emission inventory, but the disaggregation methodologies are different in each case. The higher horizontal resolution and the detailed disaggregation techniques of the CALIOPE-EU system may be responsible for the better scores obtained in primary gasses.

The horizontal resolution may impact urban and industrial areas at a higher degree than rural areas. In this sense, the higher horizontal resolution of the CALIOPE-EU system may be responsible for the better scores obtained for NO_2 and SO_2. It is reasonable to think that a detailed emission inventory at a finer horizontal resolution could further improve the air quality model performances.

Another relevant issue that arises from the model comparison is the impact of vertical resolution. Models presented in this evaluation range from 3 to 20 vertical layers. It is expected that models with higher vertical resolution covering the planetary boundary layer are able to simulate the vertical mixing better, especially for NH_3 which can have very large vertical gradients close to the ground, both decreasing and increasing with height (Schaap et al., 2004a).

The performances on NO_3^- are relatively poor which suggests that uncertainties with NO_3^- are a general feature affecting most models. The partitioning information is highly relevant as the non-linear nature of NH_4NO_3 formation. The evaluation of a regional model is hampered because the partitioning between the gas and aerosol phase is hard to verify. Another source of uncertainty in modeled NO_3^- concentration is the fact that the CALIOPE-EU system, as other European CTMs, does not estimate the formation of coarse NO_3^- through reaction of HNO_3 with sea salt or dust, as indicated by measurements in polluted marine air masses (e.g. Rodríguez et al., 2002; Querol et al., 2004, 2009; Weijers et al., 2010). In contrast, better model scores are found for SO_4^{2-}. Despite the SO_2 emissions are relatively well allocated, since exact geographical locations are known from the EPER database, there are some uncertainties about the temporal and vertical disaggregation of SO_2 emissions used in

the CALIOPE system, which is based on the EMEP model (de Meij et al., 2006; Pregger and Friedrich, 2009; Bieser et al., 2011a).

The evaluation results of this study suggest several points for future research devoted to this topic, which are presently being implemented:

- A better characterization of NH_3temporal disaggregation factors.
- An increase of the spatial coverage and reliability of data sets on NO_3^-, HNO_3, NH_3 and NH_4^+, which allow a full evaluation of photochemical model results, by means of establishing new measurements sites and systems such as the DELTA (Tang et al., 2009) and the MARGA (ten Brink et al., 1997; Thomas et al., 2009).
- Testing the ISORROPIA thermodynamic equilibrium on a daily cycle.
- Implementation of the formation of coarse NO_3^- through reaction of HNO_3 with sea salt or dust.
- Implement an update version of the chemical mechanism CB05.
- Implement biomass burning and natural emissions (e.g. lightnings, soils) which could contribute to improve the characterization of SIAs and their gaseous precursors.
- Improve vertical disaggregation profiles for anthropogenic emissions.

The model evaluation in terms of SIA indicators suggests that the CALIOPE-EU system is appropriate for regulatory modeling applications. Modeled and observed *S*-ratios indicates that fresh sulfur dominate eastern Europe, western Iberian Peninsula, and the major shipping routes, where oxidants are limiting the formation of sulfate. On the other hand, central Europe and the Mediterranean Basin are regions affected by the secondary SO_4^{2-} transported from the aforementioned emissions. NO_3^- formation is mostly limited by the availability of HNO_3 over continental region in Europe. Based on the analysis of the three studied indicators (*S*-ratio, F-NH_x and *G*-ratio) formation of SIA in Europe tends to be limited by SO_2 and HNO_3 gaseous precursors due to the relatively high NH_3 emissions, mainly from agriculture, especially in northwestern Europe. Regulatory strategies in this part of Europe could be focused on the reduction of NO_x and SO_2 rather than in NH_3 to control ammonium nitrate and ammonium sulfate, respectively. The reduction of secondary PM needs international agreements, as it is a long-range transport problem.

Acknowledgements

The authors wish to thank EMEP for the provision of measurements stations. This work is funded by the CALIOPE project of the Spanish Ministry of the Environment (441/2006/3-12.1, A357/2007/2-12.1, 157/PC08/3-12.0) and the project CICYT CGL2006-11879 and CGL2008-02818 of the Spanish Ministry of Education and Science. P. Jiménez-Guerrero acknowledges the Ramón y Cajal Programme of the Spanish Ministry of Science and Technology. The Spanish Ministry of Science and Innovation is also thanked for the Formación de Personal Investigador (FPI) doctoral fellowship held by María Teresa Pay (CGL2006-08903). We also acknowledge Dr. O. Jorba for the meteorological inputs and evaluations. All simulations were performed on the Mare Nostrum supercomputer hosted by the Barcelona Supercomputing Center.

Appendix. Supplementary data

Supplementary data associated with this article can be found in the online version, at doi:10.1016/j.atmosenv.2012.01.027.

References

Adams, P.J., Seinfeld, J.H., Koch, D.M., 1999. Global concentrations of tropospheric sulfate, nitrate, and ammonium aerosol simulated in a general circulation model. J. Geophys. Res. 104, 13791–13823.
Altshüller, A.P., 1984. Atmospheric particle sulfur and sulfur dioxide relationships at urban and nonurban locations. Atmos. Environ. 18, 1421–1431.
Ansari, A.S., Pandis, S., 1998. Response of inorganic PM to precursor concentrations. Environ. Sci. Technol. 32, 2706–2714.
Appel, K.W., Bhave, P.V., Gilliland, A.B., Sarwar, G., Roselle, S.J., 2008. Evaluation of the community multiscale air quality (CMAQ) model version 4.5: sensitivities impacting model performance; Part II-particulate matter. Atmos. Environ. 42, 6057–6066.
Asman, W.A.H., 2001. Modelling the atmospheric transport and deposition of ammonia and ammonium: an overview with special reference to Denmark. Atmos. Environ. 35, 1969–1983.
Athanasopoulou, E., Tombrou, M., Pandis, S.N., Russell, A.G., 2008. The role of sea-salt emissions and heterogeneous chemistry in the air quality of polluted coastal areas. Atmos. Chem. Phys. 8, 5755–5769.
Baldasano, J.M., Jiménez-Guerrero, P., Jorba, O., Pérez, C., López, E., Güereca, P., Martín, F., Vivanco, M.G., Palomino, I., Querol, X., Pandolfi, M.J., Sanz, M., Diéguez, J.J., 2008a. Caliope: an operational air quality forecasting system for the Iberian Peninsula, Balearic islands and Canary islands – first annual evaluation and ongoing developments. Adv. Sci. Res. 2, 89–98.
Baldasano, J.M., Güereca, L.P., López, E., Gassó, S., Jimenez-Guerrero, P., 2008b. Development of a high-resolution (1 km x 1 km, 1 h) emission model for Spain: the High-Elective Resolution Modelling Emission System (HERMES). Atmos. Environ. 42 (31), 7215–7233.
Baldasano, J.M., Pay, M.T., Jorba, O., Gassó, S., Jiménez-Guerrero, P., 2011. An annual assessment of air quality with the CALIOPE modeling system over Spain. Sci. Total Environ. 409, 2163–2178.
Baker, K., Scheff, P., 2007. Photochemical model performance for PM2.5 sulfate, nitrate, ammonium, and precursor species SO_2, HNO_3, and NH_3 at background monitor locations in the central and eastern United States. Atmos. Environ. 41, 6185–6195.
Bhave, P., Nolte, C., Pleim, J.E., Schwede, D., Roselle, S.J., 2005. Recent developments in the CMAQ modal aerosol module. In: The 2005 Models-3 Users Workshop, Chapel Hill, NC, 26–28 September 2005. Available at: http://www.cmascenter.org/conference/2005/ppt/p17.pdf.
Bieser, J., Aulinger, A., Matthias, V., Quante, M., Denier van der Gon, H.A.C., 2011a. Vertical emission profiles for Europe based on plume rise calculations. Environ. Pollut. doi:10.1016/j.envpol.2011.04.030.
Bieser, J., Aulinger, A., Matthias, V., Quante, M., Builtjes, P., 2011b. SMOKE for Europe-adaptation, modification and evaluation of a comprehensive emission model for Europe. Geosci. Model Dev. 4, 47–68.
Binkowski, F., Shankar, U., 1995. The regional particulate matter model 1.Model description and preliminary results. J. Geophys. Res. 100 (D12), 26191–26209.
Binkowski, F.S., Roselle, S.J., 2003. Models-3 Community Multiscale Air Quality (CMAQ) model aerosol component: 1. Model description. J. Geophys. Res. 108 (D16), 4183.
Boylan, J.W., Russell, A.G., 2006. PM and light extinction model performance metrics, goals, and criteria for three-dimensional air quality models. Atmos. Environ. 40 (26), 4946–4959.
Bytnerowicz, A., Omasa, K., Paoletti, E., 2007. Integrated effects of air pollution and climate change on forests: a northern hemisphere perspective. Environ. Pollut. 147, 438–445.
Byun, D., Schere, K.L., 2006. Review of the governing equations, computational algorithms, and other components of the models-3 community multiscales air quality (CMAQ) modeling system. Appl. Mech. Rev. 59 (2), 51–77.
de Meij, A., Krol, M., Dentener, F., Vignati, E., Cuvelier, C., Thunis, P., 2006. The sensitivity of aerosol in Europe to two different emission inventories and temporal distribution of emissions. Atmos. Chem. Phys. 6, 4287–4309. doi:10.5194/acp-6-4287-2006.
de Meij, A., Thunis, P., Bessagnet, B., Cuvelier, C., 2009. The sensitivity of the CHIMERE model to emissions reduction scenarios on air quality in Northern Italy. Atmos. Environ. 43, 1897–1907.
Dennis, R., Fox, T., Fuentes, M., Gilliland, A., Hanna, S., Hogrefe, C., Irwin, J., Rao, S.T., Scheffe, R., Schere, K., Steyn, D., Venkatram, A., 2010. A framework for evaluating regional-scale numerical photochemical modeling systems. Environ. Fluid Mech. doi:10.1007/s10652-009-9163-2.
EEA, 2000. CORINE Land Cover, 2000. Technical Report. European Environmental Agency. Available at: http://dataservice.eea.eu.int/dataservice.
EMEP, 2004. EMEP assessment Part I. In: Lövblad, G., Tarrasón, L., Torseth, K., Dutchak, S. (Eds.), European Perspective. Available at: www.emep.int.
European Commission, 2008. Directive 2008/50/EC of the European Parliament and of the Council of 21 May 2008 on ambient air quality and cleaner air for Europe. Technical Report 2008/50/EC, L152. Off. J. Eur. Commun.
Fagerli, H., Aas, W., 2008. Trends of nitrogen in air and precipitation: model results and observations at EMEP sites in Europe, 1980–2003. Environ. Pollut. 154, 448–461.
Fountoukis, C., Nenes, A., 2007. ISORROPIA II: a computationally efficient thermodynamic equilibrium model for K^+–Ca_2^+–Mg_2^+–NH_4^+–Na^+–SO_4^{2-}–NO_3^-–Cl^-–H_2O aerosols. Atmos. Chem. Phys. 7, 4639–4659.
Gery, M.W., Whitten, G.Z., Killus, J.P., Dodge, M.C., 1989. A photochemical kinetics mechanism for urban and regional scale computer modeling. J. Geophys. Res. 94 (D10), 12925–12956.

Gilliland, A.B., Dennis, R.L., Roselle, S.J., Pierce, T.E., 2003. Seasonal NH_3 emission estimates for the eastern United States based on ammonium wet concentrations and an inverse modeling method. J. Geophys. Res. 108 (D15), 4477. doi:10.1029/2002JD003063.

Gonçalves, M., Jiménez-Guerrero, P., López, E., Baldasano, J.M., 2008. Air quality models sensitivity to on-road traffic speed representations: effects on air quality of 80 km h^{-1} speed limit in the Barcelona Metropolitan area. Atmos. Environ. 42, 8389–8402.

Gonçalves, M., Jiménez-Guerrero, P., Baldasano, J.M., 2009a. Contribution of atmospheric processes affecting the dynamics of air pollutions in South-Western Europe during a typical summertime photochemical episode. Atmos. Chem. Phys. 9, 849–864.

Gonçalves, M., Jiménez-Guerrero, P., Baldasano, J.M., 2009b. High-resolution modeling of the effects of alternative fuels use on urban air quality: introduction of natural gas vehicles in Barcelona and Madrid Greater Areas (Spain). Sci. Total Environ. 407, 776–790.

Hamed, A., Birmili, W., Joutsensaari, J., Mikkonen, S., Asmi, A., Wehner, B., Spindler, G., Jaatinen, A., Wiedensohler, A., Korhonen, H., Lehtinen, K.E., Laaksonen, A., 2010. Changes in the production rate of secondary aerosol particles in Central Europe in view of decreasing SO_2 emissions between 1996 and 2006. Atmos. Chem. Phys. 10, 1071–1091.

Hass, H., van Loon, M., Kessler, C., Stern, R., Matthijsen, J., Sauter, F., Zlatev, Z., Langner, J., Foltescu, V., Schaap, M., 2003. Aerosol modeling: results and intercomparison from European Regional Scale Modeling System. Technical Report EUROTRAC 2 Report, EUREKA Environmental Project, GLOREAM.

Hinneburg, D., Renner, E., Wolke, R., 2007. Formation of secondary inorganic aerosols by power plant emissions exhausted through cooling towers in Saxony. Environ. Sci. Pollut. Res. 16, 25–35.

IPCC, 2007. Climate Change 2007: The Physical Science Basis. Contribution of Working Group I to the Fourth Assessment Report of the IPCC (ISBN: 978 0521 88009-1 Hardback; 978 0521 70596-7 Paperback).

Jiménez, P., Baldasano, J.M., Dabdub, D., 2003. Comparison of photochemical mechanisms for air quality modeling. Atmos. Environ. 37 (30), 4179–4194. doi:10.1016/S1352-2310(03)00567-3.

Jiménez, P., Parra, R., Gassó, S., Baldasano, J.M., 2005a. Modeling the ozone weekend effect in very complex terrains: a case study in the northeastern Iberian Peninsula. Atmos. Environ. 39, 429–444.

Jiménez, P., Jorba, O., Parra, R., Baldasano, J.M., 2005b. Influence of high-model grid resolution on photochemical modeling in very complex terrains. Int. J. Environ. Pollut. 24, 180–200.

Jiménez, P., Jorba, O., Parra, R., Baldasano, J.M., 2006a. Evaluation of MM5-EMICAT2000-CMAQ performance and sensitivity in complex terrain: high-resolution application to the northeastern Iberian Peninsula. Atmos. Environ. 40, 5056–5072.

Jiménez, P., Lelieved, J., Baldasano, J.M., 2006b. Multi-scale modeling of air pollutants dynamics in the northwestern Mediterranean basin during a typical summertime episode. J. Geophys. Res. 111 (D18306), 1–21. doi:10.1029/2005JD006516.

Jiménez, P., Parra, R., Baldasano, J.M., 2007. Influence of initial and boundary conditions for ozone modeling in very complex terrains: a case study in the northeastern Iberian Peninsula. Environ. Modell. Softw. 22, 1294–1306.

Jiménez-Guerrero, P., Pérez, C., Jorba, O., Baldasano, J.M., 2008a. Contribution of Saharan dust in an integrated air quality system and its on-line assessment. Geophys. Res. Lett. 35 (L03814). doi:10.1029/2007GL031580.

Jiménez-Guerrero, P., Jorba, O., Baldasano, J.M., Gassó, S., 2008b. The use of a modelling system as a tool for air quality management: annual high resolution simulation and evaluation. Sci. Total Environ. 390, 323–340.

Kasibhatla, P., Chameides, W.L., Jonn, J.S., 1997. A three dimensional global model investigation of seasonal variations in the atmospheric burden of anthropogenic sulphate aerosols. J. Geophys. Res. 102, 3737–3759.

Kelly, J.T., Bhave, P.V., Nolte, C.G., Shankar, U., Foley, K.M., 2010. Simulating emission and chemical evolution of coarse sea-salt particles in the Community Multiscale Air Quality (CMAQ) model. Geosci. Model Dev. 3, 257–273. doi:10.5194/gmd-3-257-2010.

Kim, Y., Sartelet, K., Seigneur, C., 2011. Formation of secondary aerosols over Europe: comparison of two gas-phase chemical mechanisms. Atmos. Chem. Phys. 11, 538–598.

Langner, J., Andersson, C., Engardt, M., 2009. Atmospheric input of nitrogen to the Baltic Sea basin: present situation, variability due to meteorology and impact of climate change. Boreal Environ. Res. 14, 226–237.

Matthias, V., 2008. The aerosol distribution in Europe derived with the Community Multiscale Air Quality (CMAQ) model: comparison to near surface in situ and sunphotometer measurements. Atmos. Chem. Phys. 8, 5077–5097.

Menut, L., Bessagnet, B., 2010. Atmospheric composition forecasting in Europe. Ann. Geophys. 28, 61–74.

Metzger, S.M., Dentener, F.J., Lelieveld, J., Pandis, S.N., 2002. Gas/aerosol partitioning I: a computationally efficient model. J. Geophys. Res. 107, 109–132.

Michalakes, J., Dudhia, J., Gill, D., Henderson, T., Klemp, J., Skamarock, W., Wang, W., 2004. The weather research and forecast model: software architecture and performance. In: Mozdzynski, E.G. (Ed.), To Appear in Proceeding of the Eleventh ECMWF Workshop on the Use of High Performance Computing in Meteorology, 25–29 October 2004, Reading, UK, pp. 117–124.

Nenes, A., Pilinis, C., Pandis, S.N., 1999. Continued development and testing of a new thermodynamic aerosol module for urban and regional air quality models. Atmos. Environ. 33, 1553–1560.

Nenes, A., Pilinis, C., Pandis, S.N., 1998. ISORROPIA: a new thermodynamic equilibrium model for multiphase multicomponent inorganic aerosols. Aquat. Geochem. 4 (1), 123–152. doi:10.1023/A:1009604003981.

Niyogi, D., Chang, H.I., Saxena, V.K., Holt, T., Alapaty, K., Booker, F., Chen, F., Davis, K.F., Holben, B., Matsui, T., Meyers, T., Oechel, W.C., Pielke, R.A., Wells, R., Wilson, K., Xue, Y., 2004. Directs observations of the effects of aerosol loading on net ecosystem CO_2 exchanges over different landscapes. Geo. Res. Lett. 31. doi:10.1029/2004GL020915.

Pay, M.T., Piot, M., Jorba, O., Gassó, S., Gonçalves, M., Basart, S., Dabdub, D., Jiménez-Guerrero, P., Baldasano, J.M., 2010a. A full year evaluation of the CALIOPE-EU air quality modeling system over Europe for 2004. Atmos. Environ. 44, 3322–3342.

Pay, M.T., Jiménez-Guerrero, P., Baldasano, J.M., 2010b. Implementation of resuspension from paved roads for the improvement of CALIOPE air quality system in Spain. Atmos. Environ. 45, 802–807. doi:10.1016/j.atmosenv.2010.10.032.

Pinder, R.W., Dennis, R.L., Bhave, P.V., 2008. Observable indicators of the sensitivity of PM2.5 nitrate to emission reductions-Part I: Derivation of the adjusted gas ratio and applicability at regulatory-relevant time scales. Atmos. Environ. 42, 1275–1286.

Piot, M., Jorba, O., Jiménez, P., Baldasano, J.M., 2008. The role of lateral boundary conditions and boundary layer in air quality modeling system. Eos Trans. AGU 8. H212+, Abstract A41H-0212.

Pleim, J.E., Chang, J.S., 1992. A non-local closure model for vertical missing in the convective boundary layer. Atmos. Environ. 26A, 965–981.

Pope, C.A.I., Ezzati, M., Dockery, D.W., 2009. Fine-particulate air pollution and life expectancy in the United States. N. Engl. J. Med. 360, 376–386.

Pregger, T., Friedrich, R., 2009. Effective pollutant emission heights for atmospheric transport modelling based on real-world information. Environ. Pollut. 157, 552–560.

Putaud, J.P., Raes, F., van Dingenen, R., Brüggemann, E., Facchini, M.C., Decesari, S., Fuzzi, S., Gehrig, R., Hüglin, C., Laj, P., Lorbeer, G., Maenhaut, W., Mihalopoulos, N., Müller, K., Querol, X., Rodriguez, S., Schneider, J., Spindler, G., ten Brink, H., Torsenth, K., Wiedensohler, A., 2004. A European aerosol phenomenology-2: chemical characteristics of particulate matter at kerbside, urban, rural and background sites in Europe. Atmos. Environ. 38, 2579–2595.

Putaud, J.P., van Dingenen, R., Alastuey, A., Bauer, H., Birmili, W., Cyrys, J., Flentje, H., Fuzzi, S., Gehrig, R., Hansson, H., Harrison, R., Herrmann, H., Hitzenberger, R., Hüglin, C., Jones, A., Kasper-Giebl, A., Kiss, G., Kousa, A., Kuhlbusch, T., Löschau, G., Maenhaut, W., Molnar, A., Moreno, T., Pekkanen, J., Perrino, C., Pitz, M., Puxbaum, H., Querol, X., Rodriguez, S., Salma, I., Schwarz, J., Smolik, J., Schneider, J., Spindler, G., ten Brink, H., Tursic, J., Viana, M., Wiedensohler, A., Raes, F., 2010. A European aerosol phenomenology – 3: physical and chemical characteristics of particulate matter from 60 rural, urban, and kerbside sites across Europe. Atmos. Environ. 44, 1308–1320. doi:10.1016/j.atmosenv.2009.12.011.

Querol, X., Alastuey, A., Ruiz, C.R., Artiñano, B., Hansson, H.C., Harrison, R.M., Buringh, E., ten Brink, H.M., Lutz, M., Bruckmann, P., Straehl, P., Schneider, J., 2004. Speciation and origin of PM10 and PM2.5 in selected European cities. Atmos. Environ. 38, 6547–6555.

Querol, X., Pey, J., Pandolfi, M., Alastuey, A., Cusack, M., Pérez, N., Moreno, T., Viana, M., Mihalopoulos, N., Kallos, G., Kleanthous, S., 2009. African dust contributions to mean ambient PM10 mass-levels across the Mediterranean Basin. Atmos. Environ. 43, 4266–4277.

Renner, E., Wolke, R., 2010. Modelling the formation and atmospheric transport of secondary inorganic aerosols with special attention to regions with high ammonia emissions. Atmos. Environ. 44, 1904–1912.

Rodríguez, S., Querol, X., Alastuey, A., Plana, F., 2002. Sources and processes affecting levels and composition of atmospheric aerosol in the Western Mediterranean. J. Geophys. Res. 107, 4777.

Roy, B., Mathur, R., Gilliland, A.B., Howard, S.C., 2007. A comparison of CMAQ-based aerosol properties with IMPROVE, MODIS, and AERONET data. J. Geophys. Res. 112 (D14301). doi:10.1029/2006JD008085.

Sartelet, K.N., Debry, E., Fahey, K., Roustan, Y., Tombette, M., Sportisse, B., 2007. Simulation of aerosols and gas-phase species over Europe with the POLYPHEMUS system: Part I-Model-to-data comparison for 2001. Atmos. Environ. 41, 6116–6131.

Schaap, M., van Loon, M., ten Brink, H.M., Dentener, F.J., Builtjes, P.J.H., 2004a. Secondary inorganic aerosol simulations for Europe with special attention to nitrate. Atmos. Chem. Phys. 4, 857–874.

Schaap, M., Spindler, G., Schulz, M., Acker, K., Maenhaut, W., Berner, A., Wieprecht, W., Streit, N., Müller, K., Brüggemann, E., Putaud, J.P., Puxbaum, H., Baltensperger, U., ten Brink, H.M., 2004b. Artefacts in the sampling of nitrate studied in the "INTERCOMP" campaigns of EUROTRAC-AEROSOL. Atmos. Environ. 38, 6487–6496.

Schaap, M., Otjes, R.P., Weijers, E.P., 2010. Illustrating the benefit of using hourly monitoring data on secondary inorganic aerosol and its precursors for model evaluation. Atmos. Chem. Phys. Discuss. 10, 12341–12370.

Schmidt, H., Derognat, C., Vautard, R., Beekmann, M., 2001. A comparison of simulated and observed ozone mixing ratios for the summer of 1998 in Western Europe. Atmos. Environ. 35, 6277–6297.

Seinfeld, J.H., Pandis, S.N., 1998. Atmospheric Chemistry and Physics. John Wiley, Hoboken, NJ.

Shankar, U., Bhave, P.V., Vukovich, J.M., Roselle, J.S., 2005. Implementation and initial applications of sea salt aerosol emissions and chemistry algorithms in the CMAQ v4.5-AERO4 module. In: The 2005 Models-3 Users Workshop, Chapel Hill, NC, 26–28 September 2005. Available at: http://www.cmascenter.org/conference/2005/abstracts/p7.pdf.

Simpson, D., Fagerli, H., Jonson, J.E., Tsyro, S., Wind, P., Tuovinen, J.P., 2003. Transboundary acidification and eutrophication and ground level ozone in Europe. Unified EMEP Model Description. Status Report 1, Part I.

Skamarock, W.C., Klemp, J.B., 2008. A time-split nonhydrostatic atmospheric model for weather research and forecasting applications. J. Comput. Phys. 227 (7), 3465–3485. doi:10.1016/j.jcp.2007.01037.

Soret, A., Jiménez-Guerrero, P., Baldasano, J.M., 2011. Comprehensive air quality planning for the Barcelona Metropolitan Area through traffic management. Atmos. Pollut. Res. 2, 255–266.

Stern, R., Builtjes, P., Schaap, M., Timmermans, T., Vautard, R., Hodzic, A., Memmesheimer, M., Feldmann, H., Renner, E., Wolke, R., Kerschbaumer, A., 2008. A model inter-comparison study focusing on episodes with elevated PM10 concentrations. Atmos. Environ. 42, 4567–4588.

Stockwell, W.R., Middleton, P., Chang, J.S., Tang, X., 1990. The second generation regional acid deposition model chemical mechanism for regional air quality modeling. J. Geophys. Res. 95, 16343–16367.

Stockwell, W.R., Kley, D., 1994. The Euro-RADM mechanism. A gas-phase chemical mechanism for European air quality studies, Beriche ds Forschungszentrums Jülich, 2868, Germany.

Stockwell, W.R., Kirchner, F., Khun, M., Seefeld, S., 1997. A new mechanism for regional atmospheric chemistry modeling. J. Geophys. Res. 102, 25847–25879.

Szopa, S., Foret, G., Menut, L., Cozic, A., 2009. Impact of large scale circulation on European summer surface ozone and consequences for modeling forecast. Atmos. Environ. 43, 1189–1195.

Tang, Y.S., Simmons, I., van Dijk, N., et al., 2009. European scale application of atmospheric reactive nitrogen measurements in a low-cost approach to infer dry deposition fluxes. Agr. Ecosyst. Environ 133, 183–195.

Tarrasón, L., Iversen, T., 1998. Modelling intercontinental transport of atmospheric sulphur in the northern hemisphere. Tellus B 50, 4331–4352.

Tarrasón, L., Fagerli, H., Klein, H., Simpson, D., Benedictow, A., Vestreng, V., Rigler, E., Emberson, L., Posh, M., Spranger, T., 2006. Transboundary Acidification, Eutrophication and Ground Level Ozone in Europe from 1990 to 2004. Technical Report. EMEP Status Report 1/06: to Support the Review of the Gothenburg Protocol. The Norwegian Meteorological Institute, Oslo, Norway.

Tarrasón, L., Fagerli, H., Jonson, J.E., Simpson, D., Benedictow, A., Klein, H., Vestreng, V., 2007. Transboundary Acidification, Eutrophication and Ground Level Ozone in Europe in 2005. EMEP Status Report 1/07. The Norwegian Meteorological Institute, Oslo, Norway. Available at. http://www.emep.int/publ/reports/2007/status_report_1_2007.pdf.

ten Brink, H.M., Kruisz, C., Kos, G.P., Berner, A., 1997. Composition/size of the light-scattering aerosol in the Netherlands. Atmos. Environ 31, 3955–3962.

Tesche, T.W., Morris, R., Tonnesen, G., McNally, D., Boylan, J., Brewer, P., 2006. CMAQ/CAMx annual 2002 performance evaluation over the eastern US. Atmos. Environ. 40, 4906–4919.

Thomas, R.M., Trebs, I., Otjes, R., Jongejan, P.A.C., ten Brink, H., Phillips, G., Kortner, M., Meixner, F.X., Nemitz, E., 2009. An automated analyser to measure surface-atmosphere exchange fluxes of water soluble inorganic aerosol compounds and reactive trace gases. Environ. Sci. Technol 43, 1412–1418.

Torseth, K., Hov. O., 2003. The EMEP monitoring strategy 2004–2009. Technical Report 9/2003. EMEP/CCC.

van Dingenen, R., Raes, F., Putaud, J.P., Baltensperger, U., Brüggemann, E., Charron, A., Facchini, M.C., Decesari, S., Fuzzi, S., Gehrig, R., Hansson, H.C., Harrison, R.M., Hüglin, Ch., Jones, A.M., Laj, P., Lorbeer, G., Maenhaut, W., Palmgren, F., Querol, X., Rodríguez, S., Schneider, J., ten Brink, H., Tunved, P., Torseth, K., Wehner, B., Weingartner, E., Wiedensohler, A., Wählin, P.A., 2004. European Aerosol Phenomenology I: Physical characteristics of particulate matter at kerbside, urban, rural and background sites in Europe. Atmos. Environ. 38, 2561–2577.

van Loon, M., Roemer, M.G.M., Builtjes, P.J.H., Bessagnet, B., Rouïl, L., Christensen, J., Brandt, J., Fegerli, H., Tarrasón, L., Rodgers, I., 2004. Model Inter-comparison in the framework of the review of the Unified EMEP model. TNO Report. Technical Report R2004/282. 53pp.

Vautard, R., Schaap, M., Bergström, R., Bessagnet, B., Brandt, J., Builtjes, P.J.H., Christensen, J.H., Cuvelier, C., Foltescu, V., Graff, A., Kerschbaumer, A., Krol, M., Roberts, P., Rouïl, L., Stern, R., Tarrasón, L., Thunis, P., Vignati, E., Wind, P., 2009. Skill and uncertainty of a regional air quality model ensemble. Atmos. Environ. 43, 4822–4832.

Vayenas, D.V., Takahama, S., Davidson, C.I., Pandis, S.N., 2005. Simulation of the thermodynamics and removal processes in the sulfate-ammonia-nitric acid system during winter: Implication for PM2.5 control strategies. J. Geophys. Res. 110 (D07S14). doi:10.1029/2004JD005038.

Vecchi, R., Valli, G., Fermo, P., D'Alessandro, A., Piazzalunga, A., Bernardoni, V., 2009. Organic and inorganic sampling artefacts assessment. Atmos. Environ. 43, 1713–1720.

Vidic, S., 2002. Frequency distribution of effective plume height. Internal Technical Note EMEP.

Weijers, E.P., Sahan, E., ten Brink, H.M., Schaap, M., Matthijsen, J., Otjes, R., van Arkel, F., 2010. Presence and characteristics of secondary inorganic aerosols in the Netherlands; measurements and modelling. Netherlands Research Program on Particulate Matter (BOP), PBL Report 500099006, PBL, Bilthoven, The Netherlands. Available at: www.pbl.nl.

Wu, S.Y., Hu, J.L., Zhang, Y., Aneja, V.P., 2008. Modeling atmospheric transport and fate of ammonia in North Carolina – Part II: effect of ammonia emissions of fine particulate matter formation. Atmos. Environ. 42, 3437–3451.

Yarwood, G., Rao, S., Yocke, M., Whitten, G., 2005. Updates to the carbon bond chemical mechanism: CB05 Final Report to the US EPA, RT-0400676. Available at: http://www.camx.com/publ/pdfs/BC05_Final_Report_120805.pdf.

Yu, S., Dennis, R., Roselle, S., Nenes, A., Walker, J., Eder, B., Schere, K., Swall, J., Malm, W., Robarge, W., 2005. An assessment of the ability of three-dimensional air quality models with current thermodynamic equilibrium models to predict aerosol NO_3^-. J. Geophys. Res. 110, D07S13.

Yu, S., Mathur, R., Sarwar, G., Kang, D., Tong, D., Pouliot, G., Pleim, J., 2010. Eta-CMAQ air quality forecasts for O_3 and related species using three different photochemical mechanisms (CB4, CB05, SAPRC-99): comparisons with measurements during the 2004 ICARTT study. Atmos. Chem. Phys. 10, 3001–3025.